NASA TECHNICAL NOTE

NASA TN D-2046

NASA TN D-2046

JET EFFECTS AT SUPERSONIC SPEEDS ON BASE AND AFTERBODY PRESSURES OF A MISSILE MODEL HAVING SINGLE AND MULTIPLE JETS

by Nickolai Charczenko and Clyde Hayes

Langley Research Center
Langley Station, Hampton, Va.

NATIONAL AERONAUTICS AND SPACE ADMINISTRATION • WASHINGTON, D. C. • NOVEMBER 1963

TECHNICAL NOTE D-2046

JET EFFECTS AT SUPERSONIC SPEEDS ON BASE AND AFTERBODY PRESSURES OF A MISSILE MODEL HAVING SINGLE AND MULTIPLE JETS

By Nickolai Charczenko and Clyde Hayes

Langley Research Center
Langley Station, Hampton, Va.

NATIONAL AERONAUTICS AND SPACE ADMINISTRATION

I

JET EFFECTS AT SUPERSONIC SPEEDS ON BASE AND AFTERBODY PRESSURES OF A MISSILE MODEL HAVING SINGLE AND MULTIPLE JETS

By Nickolai Charczenko and Clyde Hayes

SUMMARY

An investigation was made to determine pressure distribution on the base and the afterbody of a missile configuration with and without jet flow and incorporating one, two, three, four, and six nozzles. In addition, skirts of various types and lengths over the base of the model were investigated. The tests were performed at Mach numbers of 2.30, 2.95, 4.00, and 4.65 at angles of attack and sideslip of 0°.

For one- and two-nozzle configurations, or for a flared-afterbody configuration, changes in the jet pressure ratio had little effect on afterbody pressure coefficient at any of the test Mach numbers. Cylindrical afterbody configurations with more than two nozzles, however, led to an increase in pressure coefficient over the rearmost part of the afterbody at the higher jet pressure ratios. Nozzle arrangements enclosing portions of the base area led to large positive values of base pressure coefficient at high values of jet pressure ratio. This result was caused by jet boundary interaction, which forced exhaust gases into the base and hence radially outward between the nozzles. Skirt length or perforation, such as was used in these tests, had little or no effect on the base pressure coefficient, although flaring the skirt resulted in reduced base pressures at all test Mach numbers for a given jet pressure ratio.

INTRODUCTION

The problem of determining the pressure distribution on the afterbody and on the base of a missile is of considerable practical interest, inasmuch as, for high jet pressure ratios, a separation of the flow near the base of a missile can affect the control effectiveness of fins or of a flare located in the base region. Furthermore, the base drag can amount to a large portion of the total drag of the vehicle. In addition, at high altitudes, missiles having a cluster of two or more nozzles can encounter high heating rates at the base as a result of the reverse flow of gases entrapped between the nozzles (for example, refs. 1, 2, and 3).

To obtain a theoretical solution of base-pressure distributions for bodies of revolution at supersonic speeds is difficult, even without the jet flow; with the jet flow the problem becomes further complicated. For this reason numerous investigations have been performed to obtain experimental data to show the effects of various parameters on the base pressures. Such data have been combined in some cases, as in reference 4, and used successfully to predict missile base pressures.

The present investigation was performed to obtain experimental data on a missile configuration with and without jet flow and incorporating one, two, three, four, and six nozzles. In addition, skirts of various types and lengths over the base of the model were investigated. The tests were performed at Mach numbers of 2.30, 2.95, 4.00, and 4.65 at angles of attack and sideslip of 0°.

SYMBOLS

C_p average pressure coefficient, $\frac{p - p_\infty}{q_\infty}$

D model diameter, in.

L skirt length, measured from model base plane, in.

M Mach number

p static pressure, lb/sq ft

q dynamic pressure, lb/sq ft

R Reynolds number (based on model diameter)

r radial distance from center of base (fig. 6), in.

x longitudinal distance from end of skirt (fig. 8), in.

ϕ meridian angle (fig. 6), deg

Subscripts:

a afterbody

b base

j jet exhaust

∞ free stream

APPARATUS

Wind Tunnel

The tests were conducted in the Langley Unitary Plan wind tunnel. The test section of the tunnel is 4 by 4 feet in cross section and approximately 7 feet long. The Mach number may be varied from 2.3 to 4.65 in any desired increment without tunnel shutdown, by operating an asymmetric sliding block. Further details of the tunnel may be obtained from reference 5.

Model

The model was designed to simulate the aft end of a typical rocket booster. It was cylindrical in shape and had an outside diameter of 4 inches except for the forward 25 percent of the length which consisted of a conical nose with a rounded tip. The model was supported by a hollow strut which also served to house the high-pressure air lines leading to the simulated rocket chamber; the supporting strut also housed the pressure tubes from the pressure orifices to the Scanivalves located outside the tunnel. The general arrangement of the model and the model support system are shown in figure 1 and a photograph is shown in figure 2. Details of the model are shown in figure 3 and model photographs are shown in figure 4.

The configuration was varied by means of an interchangeable base which allowed the use of bases having one, two, three, four, and six nozzles (designated N_1, N_2, N_3, N_4, and N_6). Details and a photograph of the nozzle bases are shown in figures 5 and 6. The nozzles were designed to have equal total throat areas, fixed location of the throat-area plane, and a constant nozzle-exit angle of 10°. The nozzle area ratios were designed to provide an exit Mach number of 3.175. The orifices on the base and external surfaces of the nozzles were located as shown in figure 6.

Provision was also made for the variation of the skirt geometry at the base of the model. Solid skirts of approximately 1/4, 3/8, and 1/2 base diameter in length (designated S_1, S_2, and S_3), a perforated skirt of 3/8 base diameter (S_6), and a flared skirt of 1/4 base diameter (S_{10}) were tested. Details and a photograph of the skirt arrangements are shown in figure 7. Orifice locations for the skirts are shown in figure 8.

The following table lists the various configurations tested with the nomenclature used to indicate each combination of skirt length and number of nozzles:

Skirt length and type	Number of nozzles				
	1	2	3	4	6
$L \approx \frac{1}{4} D$, solid	S_1N_1	S_1N_2	S_1N_3	S_1N_4	S_1N_6
$L \approx \frac{3}{8} D$, solid	----	----	S_2N_3	-----	----
$L \approx \frac{1}{2} D$, solid	----	----	S_3N_3	-----	----
$L \approx \frac{1}{2} D$, perforated	----	----	S_6N_3	-----	----
$L \approx \frac{1}{4} D$, flared	----	----	----	$S_{10}N_4$	----

Instrumentation and Accuracy

Pressure measurements on the afterbody and on the base of the model were made by connecting the orifices to scanning pressure valves (Scanivalves). Five Scanivalves, with 5-pound-per-square-inch transducers, were used to reduce the required scanning time. The jet-exit pressures were measured by four individual 25-pound-per-square-inch transducers. The transducer outputs were digitized and punched into cards for machine calculation of the pressure coefficient (C_p). The free-stream and stagnation pressures were measured on precision mercury manometers, accurate to within 0.5 pound per square foot.

The maximum deviation of the free-stream Mach number in the range covered by these tests is ± 0.05. The accuracy of the quantity C_p is estimated to be within ± 0.015.

TESTS

With the angle of attack and angle of sideslip of the model set at 0° pressure coefficients were obtained for the following test conditions:

Test conditions				Configuration								
M_∞	R	q_∞, lb/sq ft	p_j/p_∞	S_1N_1	S_1N_2	S_1N_3	S_2N_3	S_3N_3	S_6N_3	S_1N_4	$S_{10}N_4$	S_1N_6
2.30	0.50×10^6	341	0 to 26	x	x	x	x	-	-	x	x	x
2.95	0.60×10^6	361	0 to 40	x	-	x	x	-	-	x	x	x
4.00	0.73×10^6	320	0 to 80	x	x	x	x	-	-	x	x	x
4.65	0.91×10^6	313	0 to 110	x	x	x	x	x	x	x	x	-

In these tests dry, high-pressure air at a stagnation temperature of approximately 70° F was used for jet simulation. During the test, pressures at each of the orifices shown in figures 6 and 8 were measured individually; however, the pressure coefficients presented in figures 9 and 10 are the average pressure coefficients for a given station x on the afterbodies, or a constant r on the model base. Similarly, the nozzle exit pressures are averages obtained from orifices located 90° apart inside the nozzle, 0.07 inch from the exit.

RESULTS AND DISCUSSION

Jet Effects on Afterbody Pressure

The effect of jet pressure ratios on afterbody pressures is presented in figure 9 for all test configurations and Mach numbers. At a Mach number of 2.30 there was little or no effect of jet pressure ratios on afterbody pressure coefficients for any of the test configurations. All pressure coefficients were slightly negative with the exception of those obtained for the flared-skirt configuration which had positive pressure coefficients. In general, there were only small differences in pressure coefficients at any of the afterbody stations investigated, although the most rearward orifice indicated slightly greater negative values. With an increase in Mach number the afterbody pressure coefficients remained essentially the same as at $M = 2.30$ for the one- and two-nozzle configurations, the flared-afterbody configuration, and the other nozzle configurations at the lower jet pressure ratios. For the cylindirical afterbody configurations with more than two nozzles, however, an increase in jet pressure ratio at higher Mach numbers led to an increase in pressure coefficients on the rearmost part of the afterbody. For example, at $M = 4.65$, configuration S_3N_3 has positive pressure coefficients for the rearmost orifice location at jet pressure ratios larger than about 40 (fig. 9(d)). The rearmost orifices on the model were located only 0.07 inch from the end of the skirt and for that reason were subjected to greater influence of the base pressure than other orifices. As a result, low base pressures led to a reduction in pressures near the end of a skirt and, conversely, high base pressures led to an increase in pressures.

Jet Effects on Base Pressure

Base pressure coefficients are presented in figure 10 as a function of jet- to free-stream static pressure ratios for the configurations and the test Mach numbers. In most instances the lowest values of p_j/p_∞ in figures 9 and 10 correspond to jet-off condition. The general trends in the variation of base pressure coefficients with p_j/p_∞ are similar to those obtained in the previous investigations (refs. 6 to 14); that is, the most negative values of base pressure coefficients were obtained at the lower jet- to free-stream pressure ratios and there was a consistent increase in base pressure as p_j/p_∞ was increased.

At a Mach number of 2.30 for the one-, two-, and six-nozzle configurations, the base-pressure distribution on the base was nearly uniform and a slight increase in the slope of $C_{p,b}$ as a function of p_j/p_∞ occurred with increase in number of nozzles (fig. 10(a)). This is believed to be primarily the result of an increase in the effective jet-to-base area ratio. For the three- and four-nozzle configurations, differences in $C_{p,b}$ for various orifice locations were appreciable, particularly at higher values of jet pressure ratio. For each of these nozzle arrangements, the highest values of $C_{p,b}$ were obtained at the center of the base, with the four-nozzle configuration having the greatest values at this location. The high pressures were caused by a reversed flow into the base region, a phenomenon that takes place at high jet pressure ratios for clustered nozzles. This phenomenon occurs when an interaction of the jets results in high local pressures which feed back into the base region; a more detailed explanation of this phenomenon is given in reference 15. From the radial pressure distribution shown in figure 11, it is apparent that for three- and four-nozzle configurations the flow proceeds radially outward between the nozzles from the high pressure region at the center. Although similar effects would be expected for the six-nozzle configuration, this result could not be established from the available pressure distributions. It could be stated that whenever the nozzle arrangement encloses portions of the base area, reverse flow into these regions will tend to occur when pressure ratios become high enough to cause jet boundary interaction. Similar effects to those noted at Mach number 2.30 were found at other Mach numbers (figs. 10(b) to (d)).

There appears to be little or no effect of the skirt length (such as the lengths used for these tests) on the base pressure coefficient. However, flaring the afterbody leads to a significant reduction in base pressure as compared with the cylindrical afterbody at all Mach numbers for a given jet pressure ratio. Data obtained at $M = 4.65$ for the perforated-skirt configuration also showed little or no effect of the perforations on base pressure coefficients (fig. 10(d)).

Figure 12 shows some typical flow fields for the multinozzle configurations for the test Mach numbers and at several jet pressure ratios.

SUMMARY OF RESULTS

Tests of a missile configuration to determine the effects of the number of nozzles, the skirt geometry, and the jet pressure ratio on afterbody and base pressure coefficients at Mach numbers from 2.30 to 4.65 indicated the following results:

1. For one- and two-nozzle configurations, or a flared-afterbody configuration, there was little effect of the jet pressure ratio on the afterbody pressure coefficient at any of the test Mach numbers. Cylindrical afterbody configurations with more than two nozzles, however, led to increases in pressure coefficients over the rearmost part of the afterbody at the higher jet pressure ratios.

2. Nozzle arrangements enclosing portions of the base area led to large positive values of base pressure coefficient at high values of jet pressure ratio. These large positive values were caused by jet boundary interaction, which forced exhaust gases into the base and thence radially outward between the nozzles.

3. Skirt length or perforation, such as used for these tests, had little or no effect on the base pressure coefficient, although flaring the skirt resulted in reduced base pressures at all test Mach numbers for a given jet pressure ratio.

Langley Research Center,
National Aeronautics and Space Administration,
Langley Station, Hampton, Va., September 4, 1963.

REFERENCES

1. Anon.: Symposium Proceedings December 1-2, 1959 - Simulated Altitude Testing of Rockets and Missile Components. AEDC-TR-60-6 (Contract No. AF 40(600)-800), Arnold Eng. Dev. Center, Mar. 1960.

2. Morris, J. A., and Cannell, A. L.: Base Recirculation of a 1/10-Scale Saturn S-IV Stage at Simulated Altitudes Above 142,000 ft. AEDC-TN-61-102 (Contract No. AF 40(600)-800 S/A 24(61-73)), Arnold Eng. Dev. Center, Aug. 1961.

3. Musial, Norman T., Ward, James J.: Base Flow Characteristics for Several Four-Clustered Rocket Configurations at Mach Numbers From 2.0 to 3.5. NASA TN D-1093, 1961.

4. Boren, T. C., and Hatalsky, William: Jet Effects Upon Base Drag. Gen. Dynamics/Pomona, [1960].

5. Anon.: Manual for Users of the Unitary Plan Wind Tunnel Facilities of the National Advisory Committee for Aeronautics. NACA, 1956.

6. Allen, John L.: Base-Flow Aerodynamics of a Saturn-Type Booster Stage at Mach Numbers 0.1 to 2.0. NASA TN D-593, 1962.

7. Beheim, Milton A., Klann, John L., and Yeager, Richard A.: Jet Effects on Annular Base Pressure and Temperature in a Supersonic Stream. NASA TR R-125, 1962.

8. Baughman, L. Eugene, and Kochendorfer, Fred D.: Jet Effects on Base Pressures of Conical Afterbodies at Mach 1.91 and 3.12. NACA RM E57E06, 1957.

9. Bromm, August F., Jr., and O'Donnell, Robert M.: Investigation at Supersonic Speeds of the Effect of Jet Mach Number and Divergence Angle of the Nozzle Upon the Pressure of the Base Annulus of a Body of Revolution. NACA RM L54I16, 1954.

10. Cubbage, James M., Jr.: Jet Effects on Base and Afterbody Pressures of a Cylindrical Afterbody at Transonic Speeds. NACA RM L56C21, 1956.

11. Cortright, Edgar M., Jr., and Kochendorfer, Fred D.: Jet Effects on Flow Over Afterbodies in Supersonic Stream. NACA RM E53H25, 1953.

12. Scott, William R., and Slocumb, Travis H., Jr.: Jet Effects on the Base Pressure of a Cylindrical Afterbody With Multiple-Jet Exits. NASA MEMO 3-10-59L, 1959.

13. Cubbage, James M., and Andrews, Earl H., Jr.: Measured Base Pressures on Several Twin Rocket-Nozzle Configurations at Mach Numbers of 0.6 to 1.4 With Effects Due to Nozzle Canting and Stabilizing Fins. NASA TN D-544, 1960.

14. Baughman, Eugene L.: Wind Tunnel Investigation at Mach 1.9 of Multijet-Missile Base Pressures. NACA RM E54L14, 1955.

15. Geothert, B. H.: Base Flow Characteristics of Missiles With Cluster-Rocket Exhausts. Paper No. 60-89, Inst. Aero. Sci., June-July 1960.

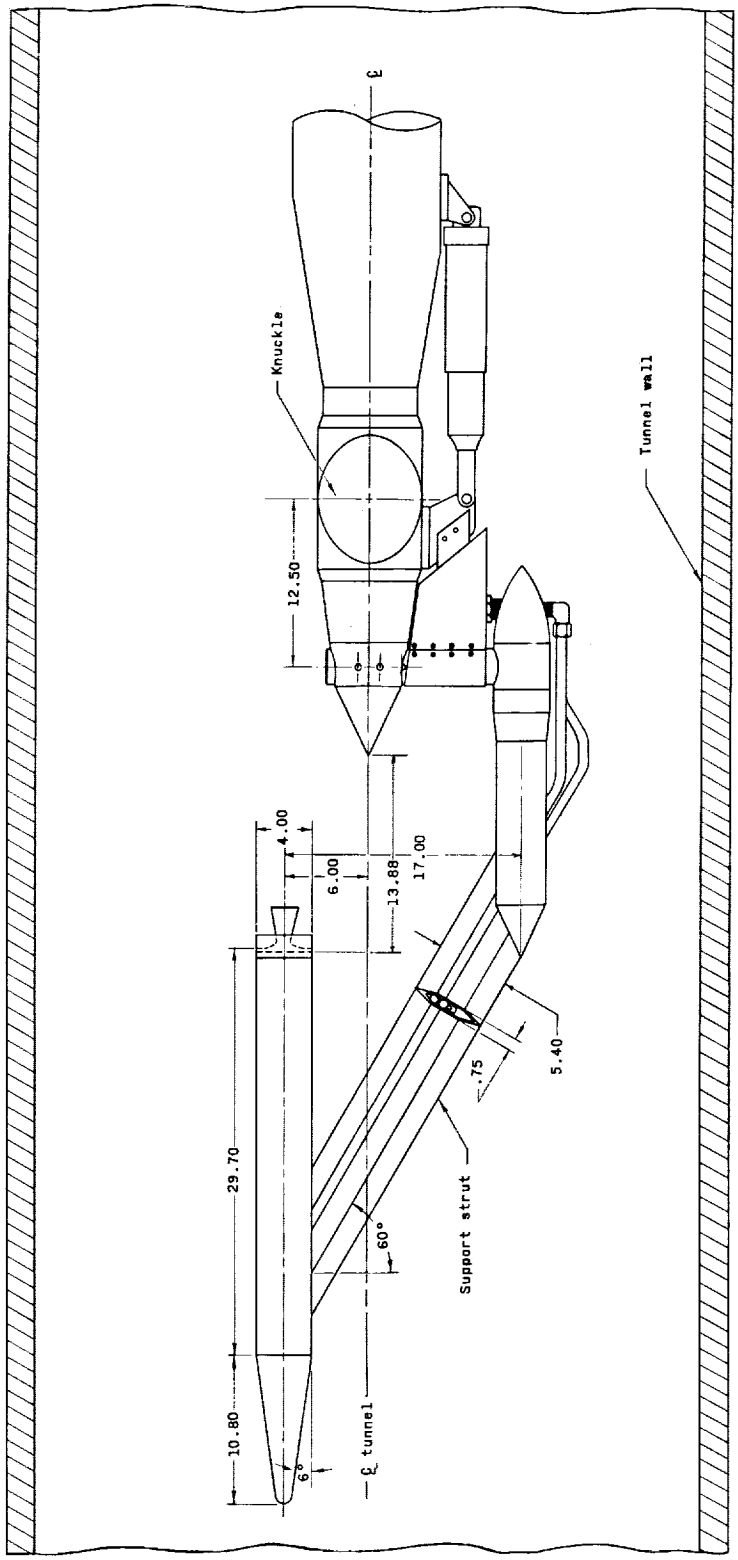

Figure 1.- Drawing of model and model-support arrangement. (Dimensions are in inches.)

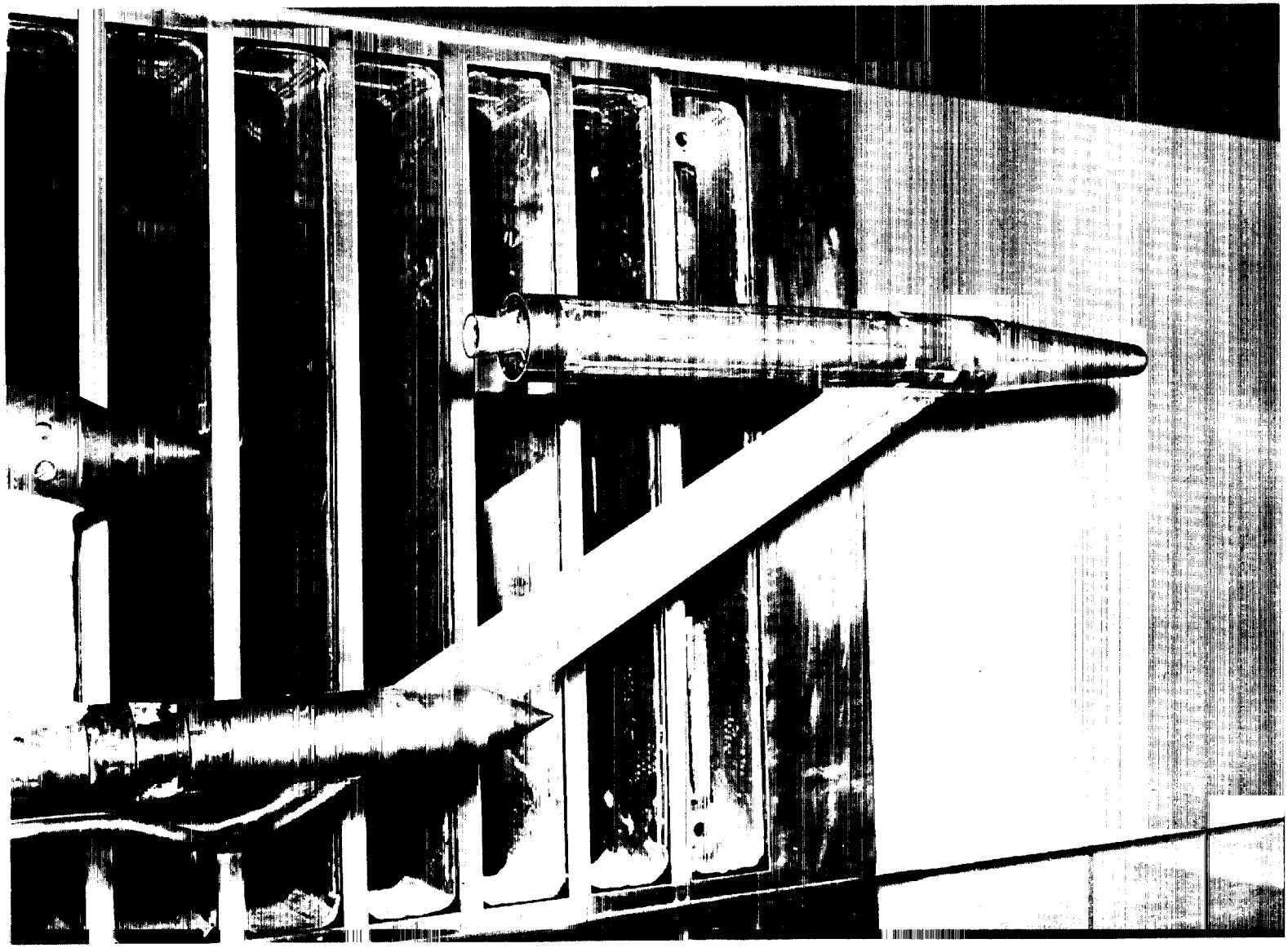

Figure 2.- Tunnel installation. L-58-1389a

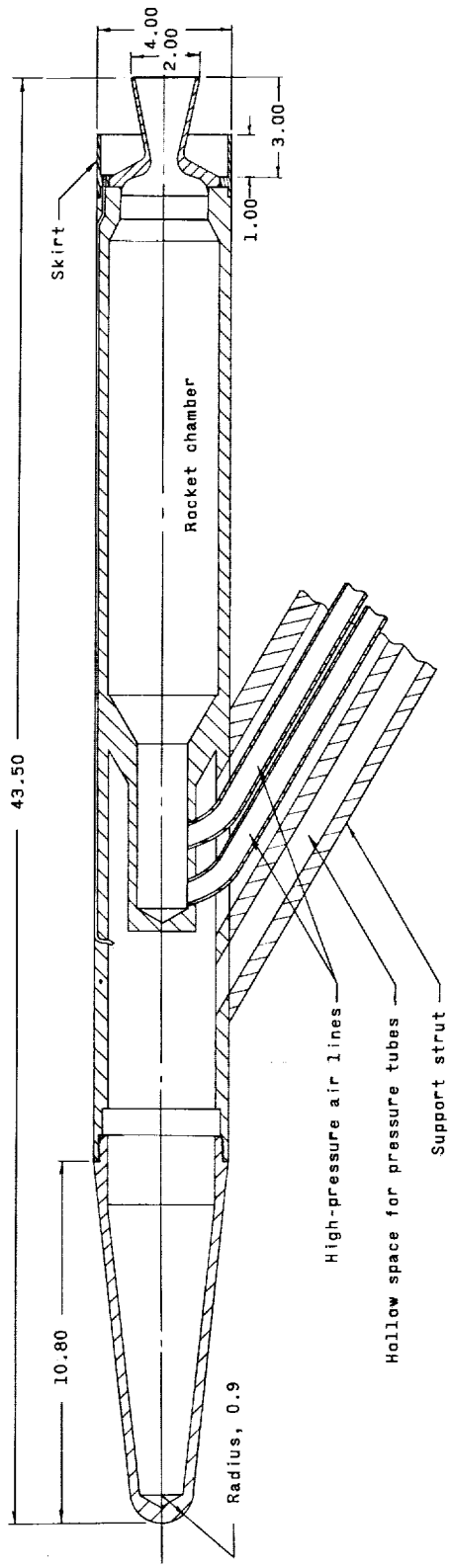

Figure 3.- Details of test model. (Dimensions are in inches.)

Single-nozzle configuration

L-60-867

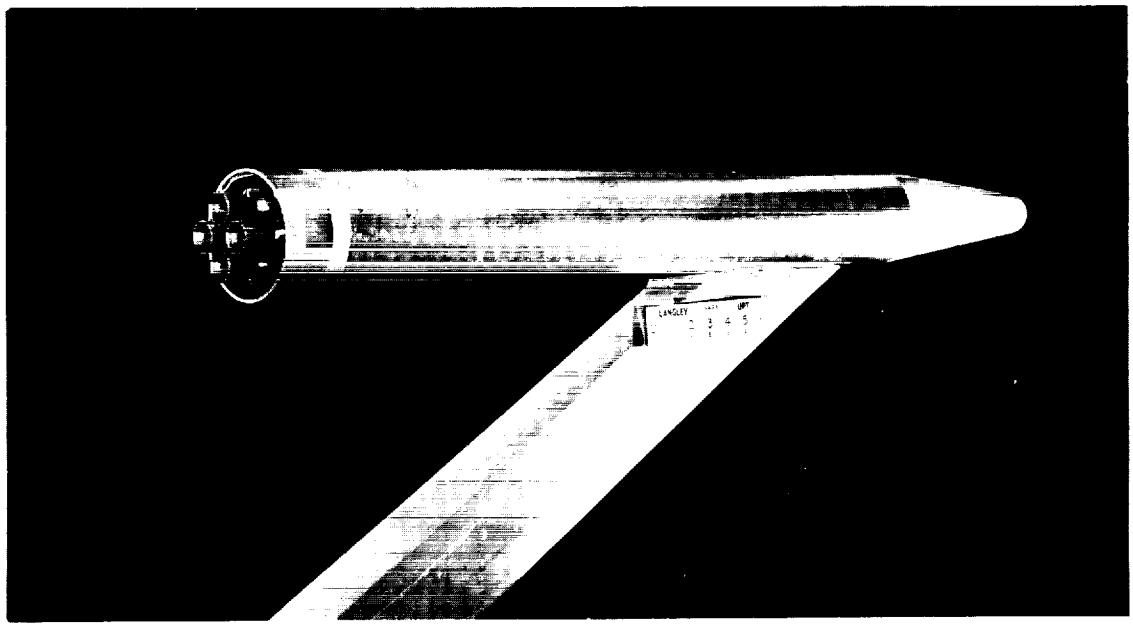

Multinozzle configuration

Figure 4.- Test model.

L-60-870

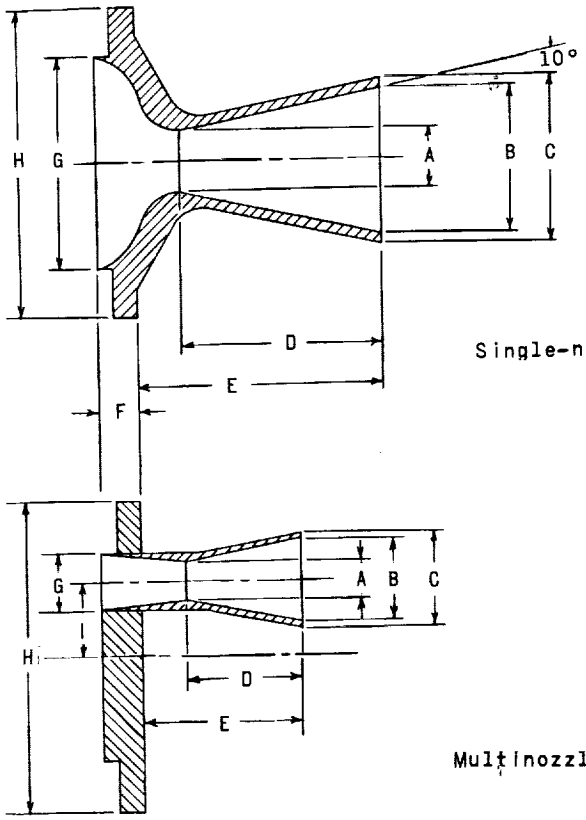

Number of nozzles	Dimensions, in.									Total throat area, sq in.
	A	B	C	D	E	F	G	H	I	
One Nozzle	0.781	1.746	2.000	2.453	3.000	0.800	2.550	3.800	0.000	0.48
Two Nozzles	.552	1.233	1.413	1.731	2.278	.500	.963	3.800	.750	.48
Three Nozzles	.451	1.009	1.157	1.417	1.964	.500	.706	3.800	.862	.48
Four Nozzles	.391	.873	1.000	1.226	1.773	.500	.800	3.800	.845	.48
Six Nozzles	.319	.713	.816	1.002	1.549	.500	.550	3.800	.940	.48

(a) Nozzle drawing.

Figure 5.- Drawing and photograph of nozzles.

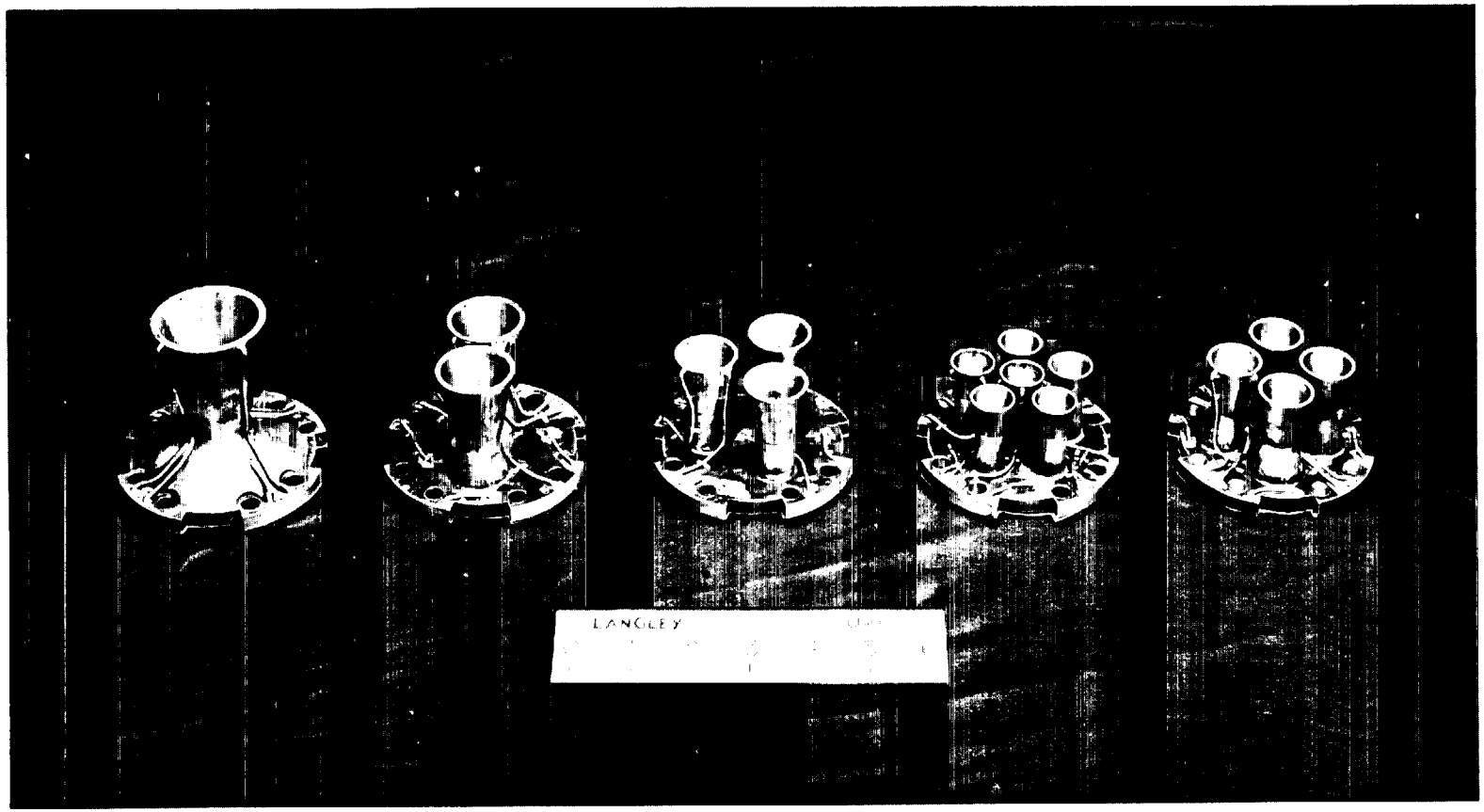

(b) Photograph of nozzles. L-60-872

Figure 5.- Concluded.

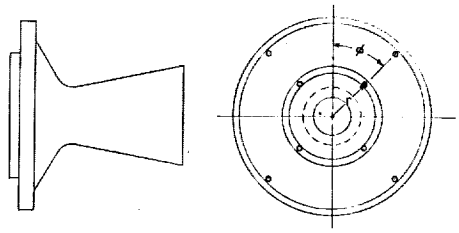

N_1

Configuration	r, in.	ϕ, deg			
		45	135	225	315
One nozzle	0.90	x	x	x	x
	1.79	x	x	x	x

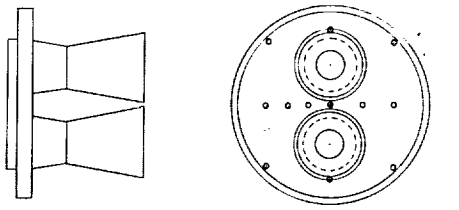

N_2

Configuration	r, in.	ϕ, deg							
		0	45	90	135	180	225	270	315
Two nozzles	0	x							
	0.43							x	
	0.64			x					
	0.85							x	
	1.28			x				x	
	1.50	x				x			
	1.79		x		x		x		x

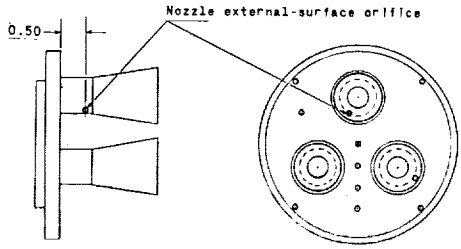

N_3

Configuration	r, in.	ϕ, deg							
		0	45	60	135	180	225	300	315
Three nozzles	0	x							
	0.43					x			
	0.87					x			
	1.31			x		x		x	
	1.79		x		x		x		x

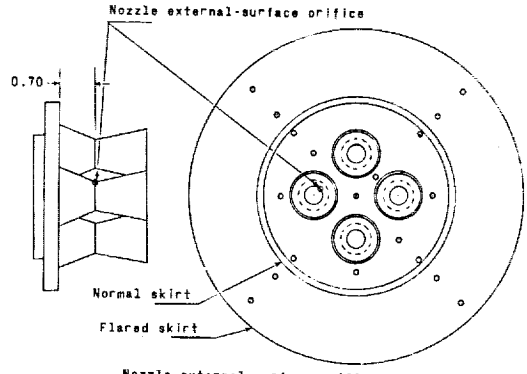

N_4

Configuration	r, in.	ϕ, deg							
		0	45	90	135	180	225	270	315
Four nozzles	0	x							
	0.54		x						
	1.22				x				x
	1.53	x		x		x		x	
	1.79		x		x		x		x
	2.30*		x		x		x		x
	3.00*		x		x		x		x

* Flared skirt configuration only

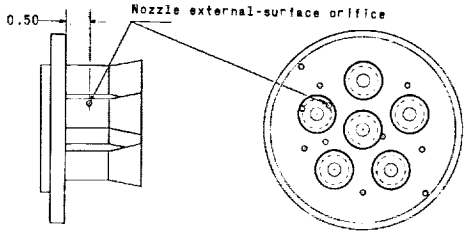

N_6

Configuration	r, in.	ϕ, deg						
		45	108	135	180	252	288	315
Six nozzles	0.41		x					
	0.80					x		
	1.25	x	x		x	x	x	x
	1.79			x				x

Figure 6.- Location of base-pressure orifices. (Dimensions are in inches.)

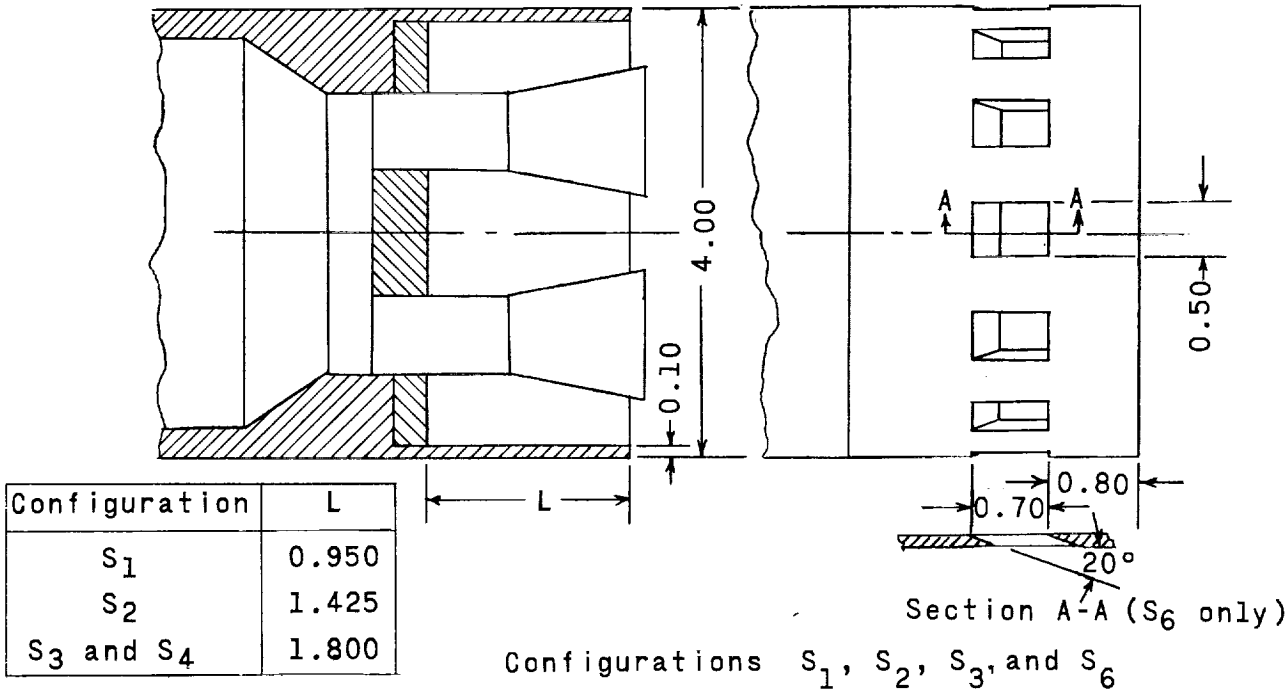

Configuration	L
S_1	0.950
S_2	1.425
S_3 and S_4	1.800

Configurations S_1, S_2, S_3, and S_6

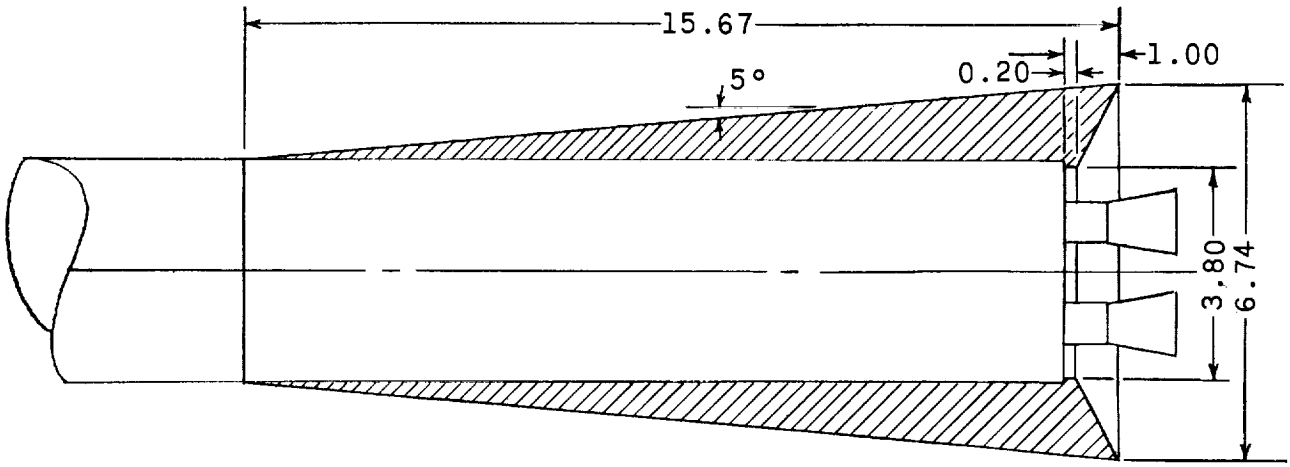

Configuration S_{10}

(a) Detailed drawing of skirts.

Figure 7.- Drawing and photograph of skirts. (Dimensions are in inches.)

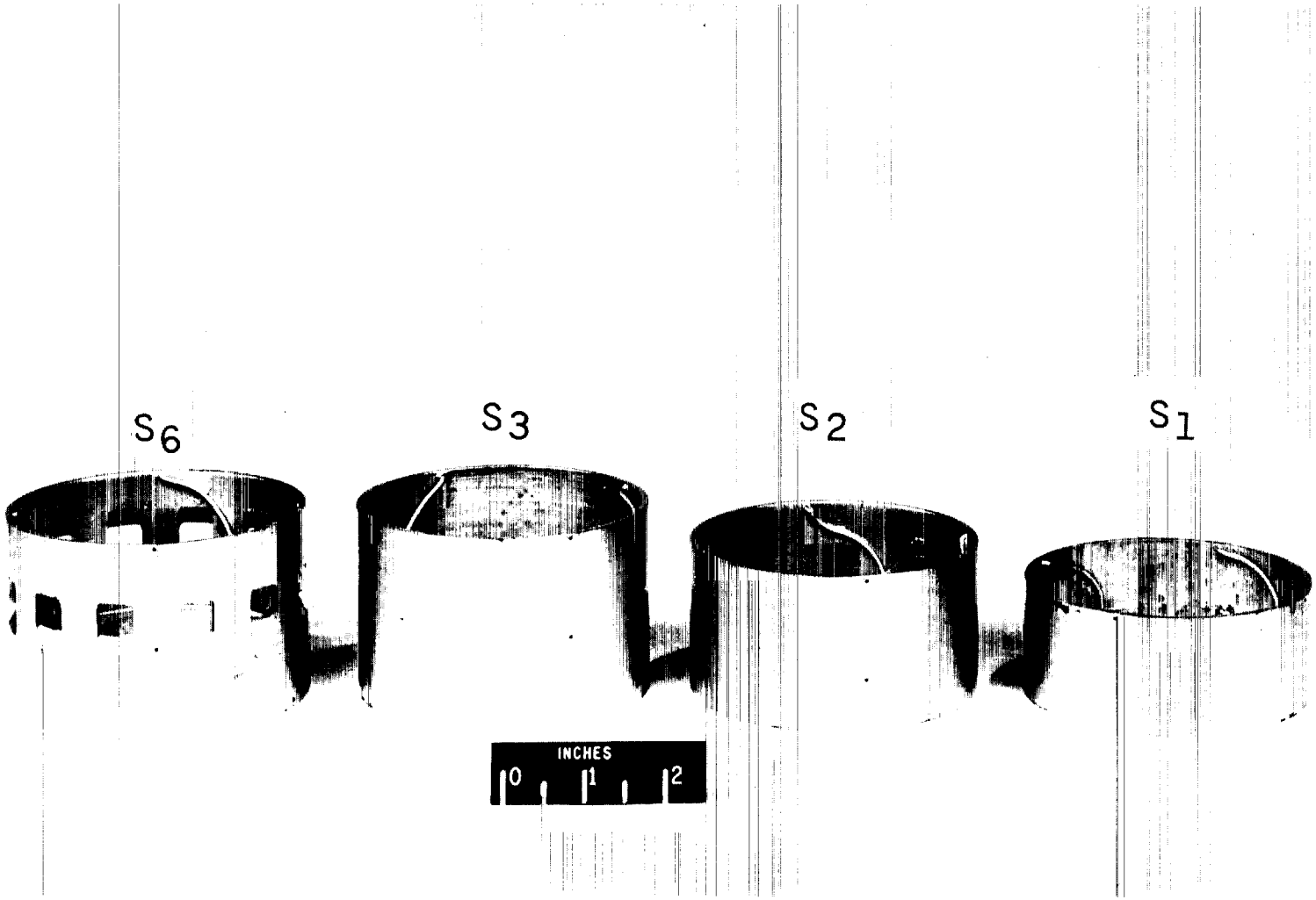

(b) Photograph of skirts. L-63-1049

Figure 7.- Concluded.

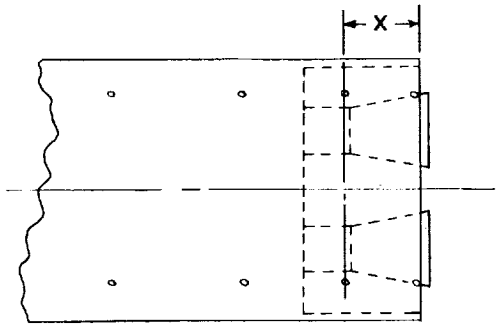

Configurations S_1, S_2, and S_3

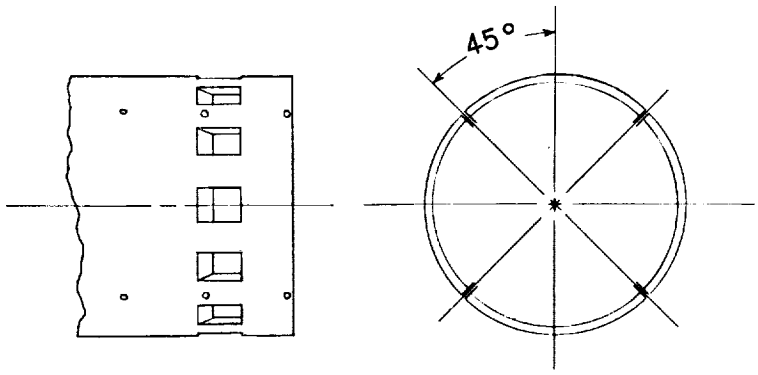

Configuration S_6

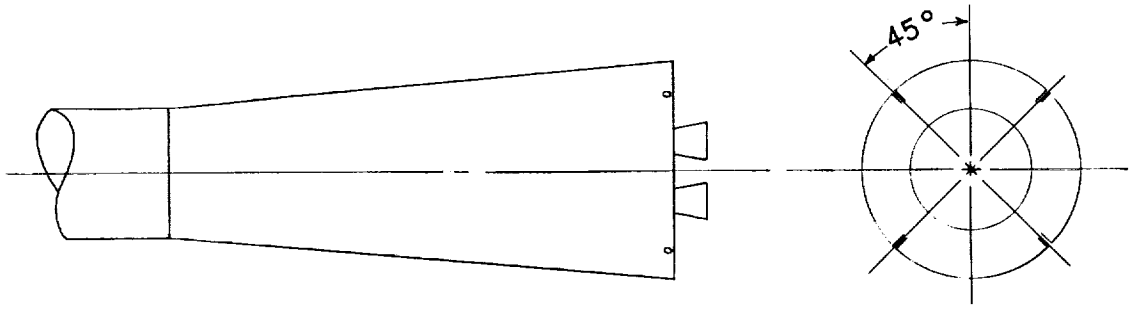

Configuration S_{10}

Configuration	x, in.			
S_1, $L \approx \frac{1}{4}D$	0.070	2.70	4.70	
S_2, $L \approx \frac{3}{8}D$	.070	1.40	3.20	5.20
S_3 and S_6, $L \approx \frac{1}{2}D$	.070	1.40	3.70	5.70
S_{10}, $L \approx \frac{1}{4}D$, flared	.070			

Figure 8.- Location of static-pressure orifices on afterbody.

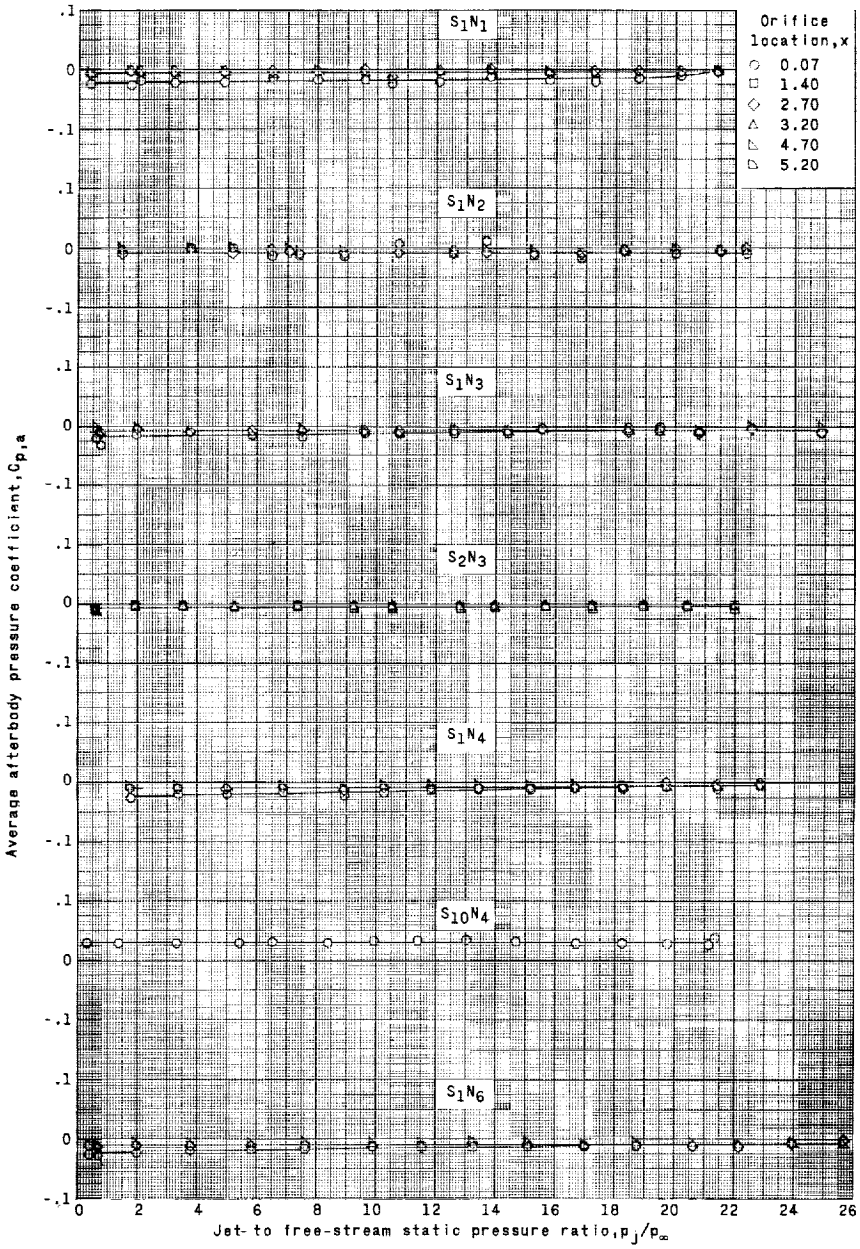

(a) $M_\infty = 2.30$.

Figure 9.- Jet effects on afterbody pressures.

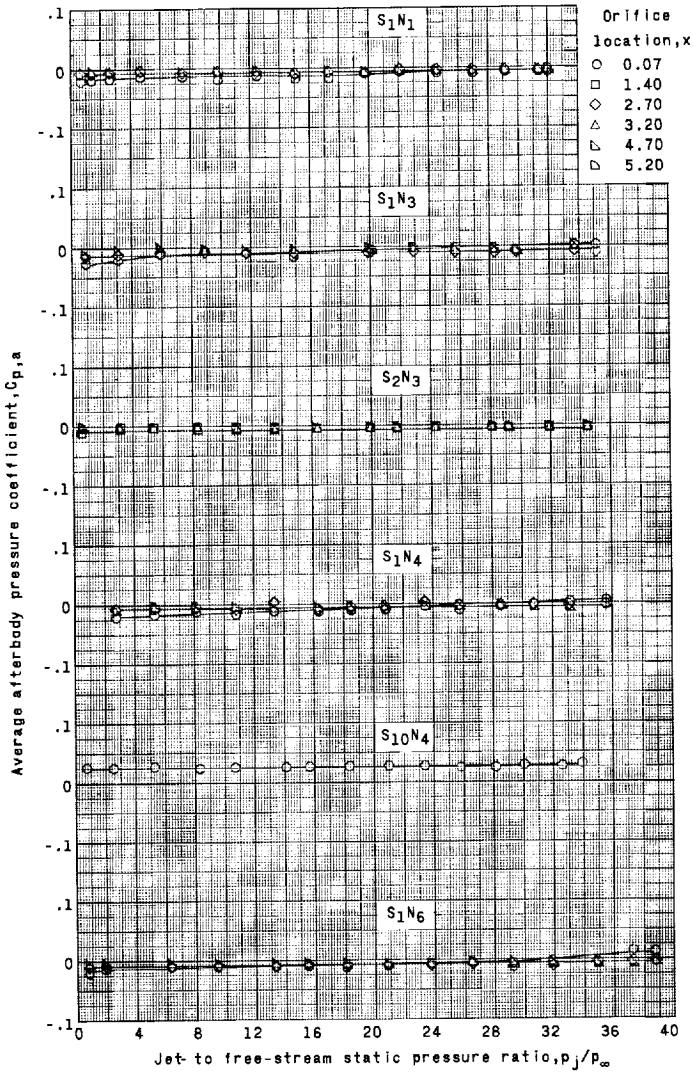

(b) $M_\infty = 2.95$.

Figure 9.- Continued.

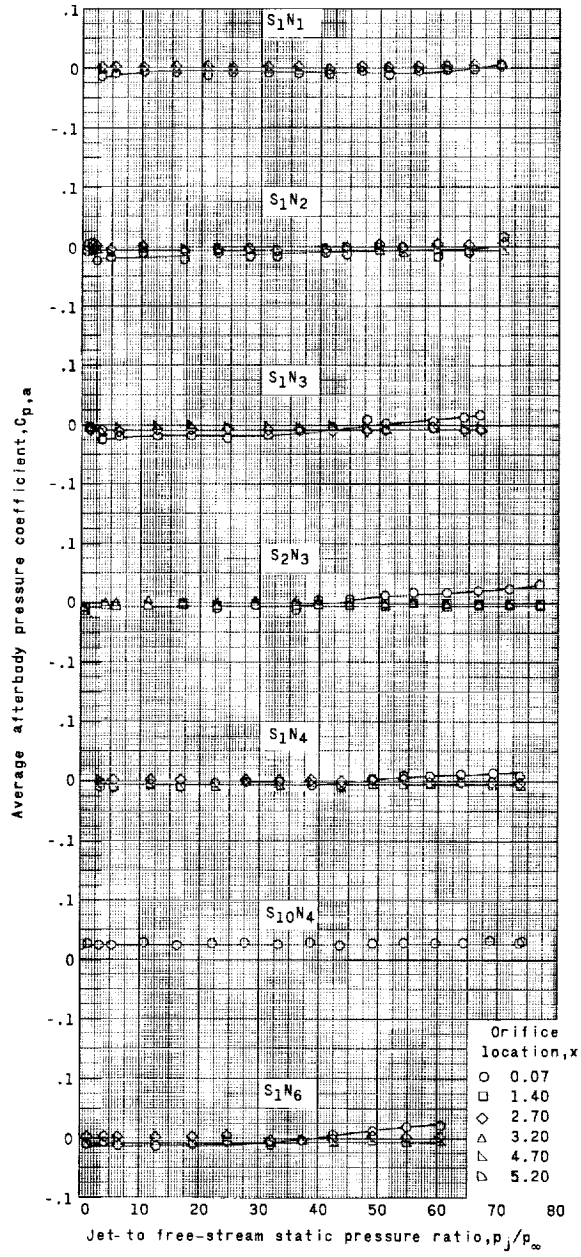

(c) $M_\infty = 4.00$.

Figure 9.- Continued.

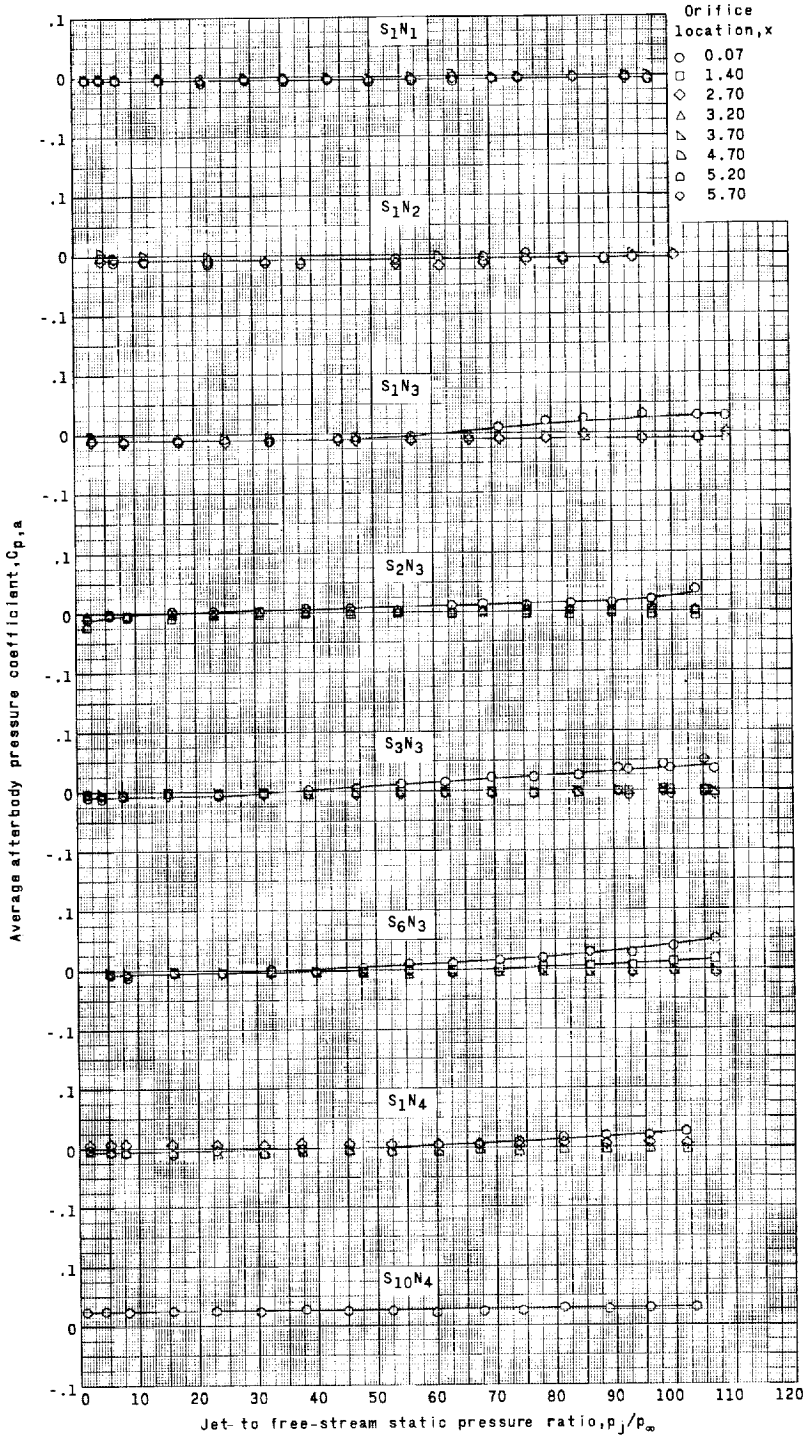

(d) $M_\infty = 4.65$.

Figure 9.- Concluded.

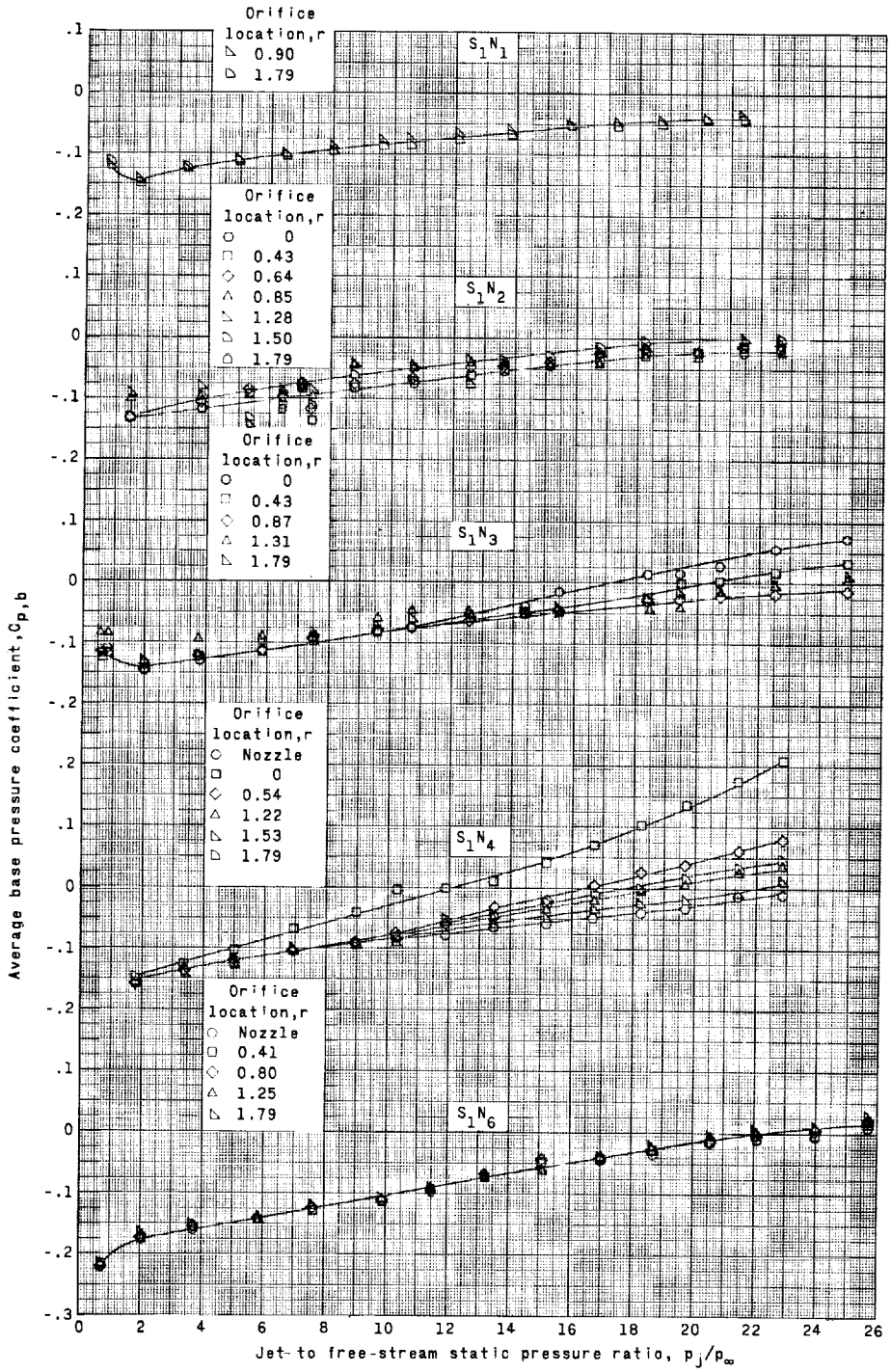

(a) $M_\infty = 2.30$.

Figure 10.- Jet effects on base pressures.

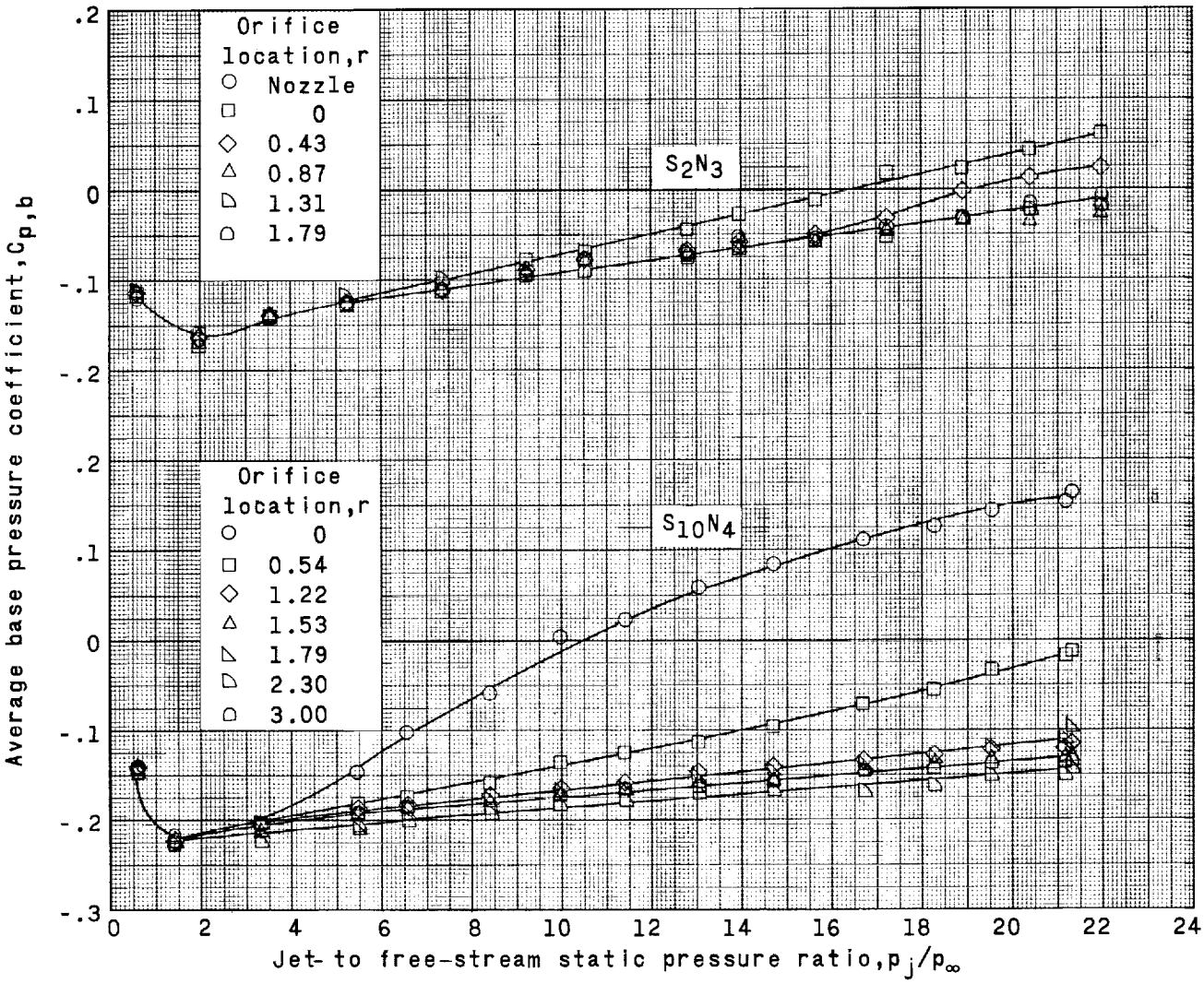

(a) Concluded.

Figure 10.- Continued.

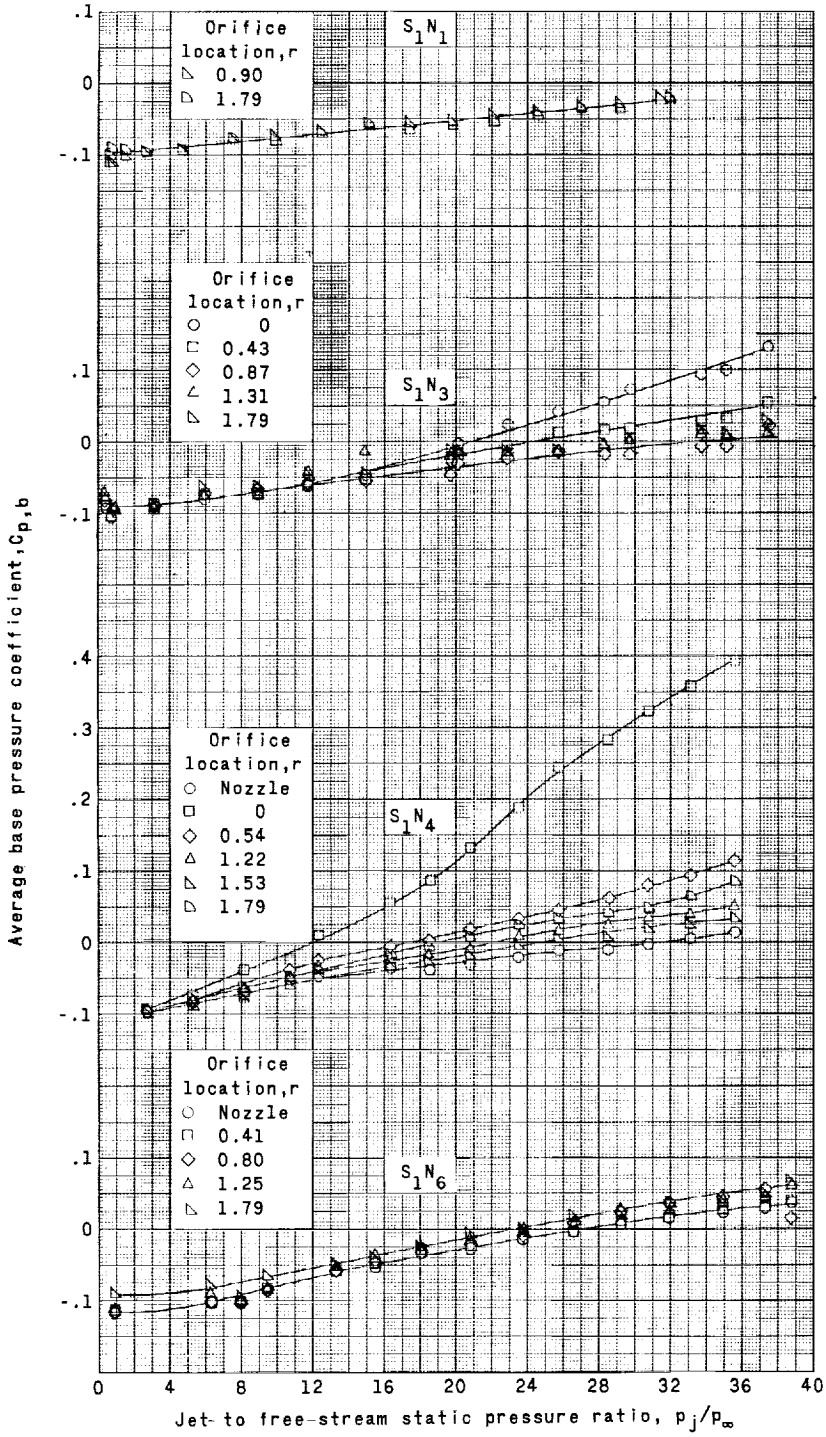

(b) $M_\infty = 2.95$.

Figure 10.- Continued.

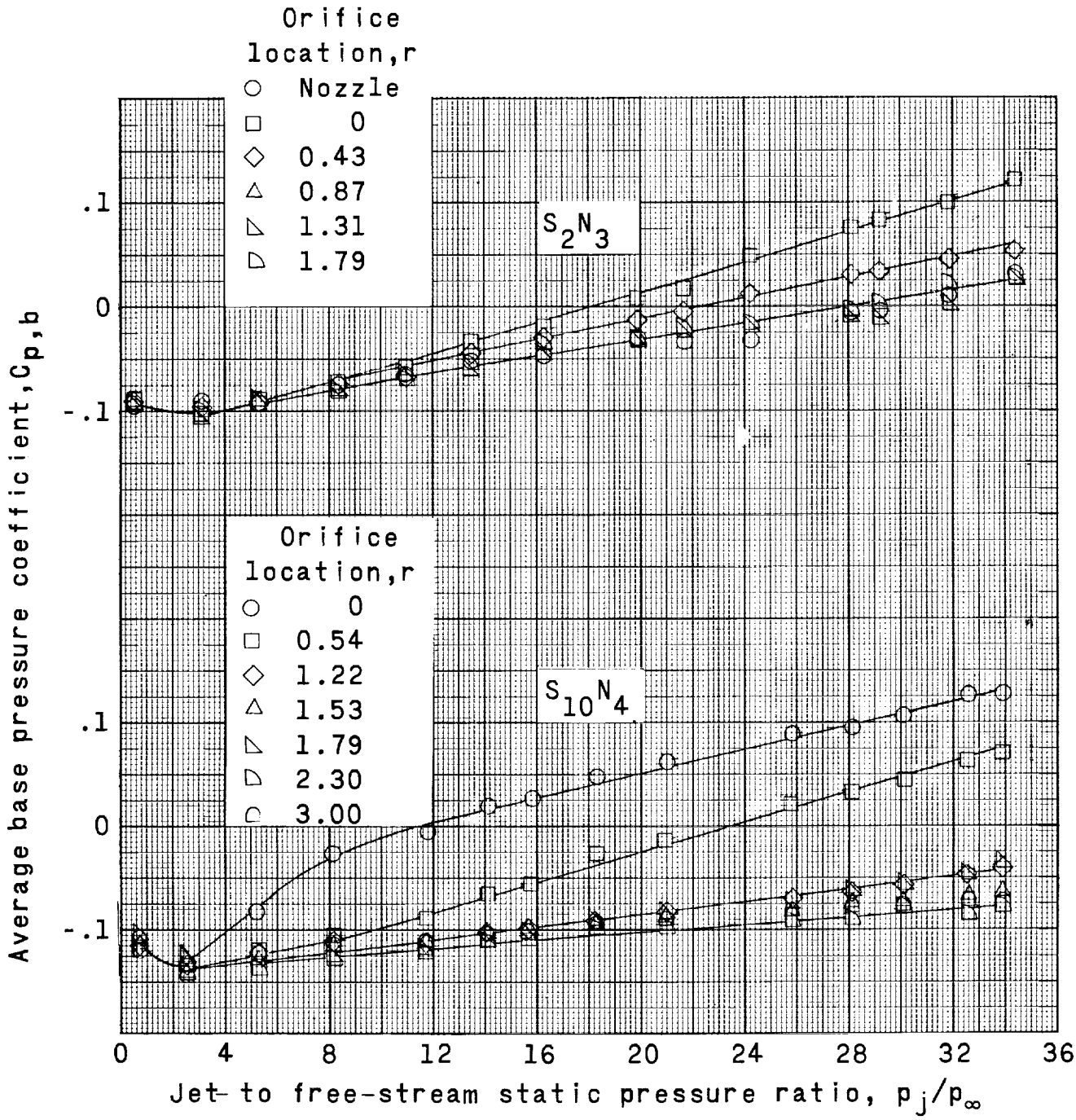

(b) Concluded.

Figure 10.- Continued.

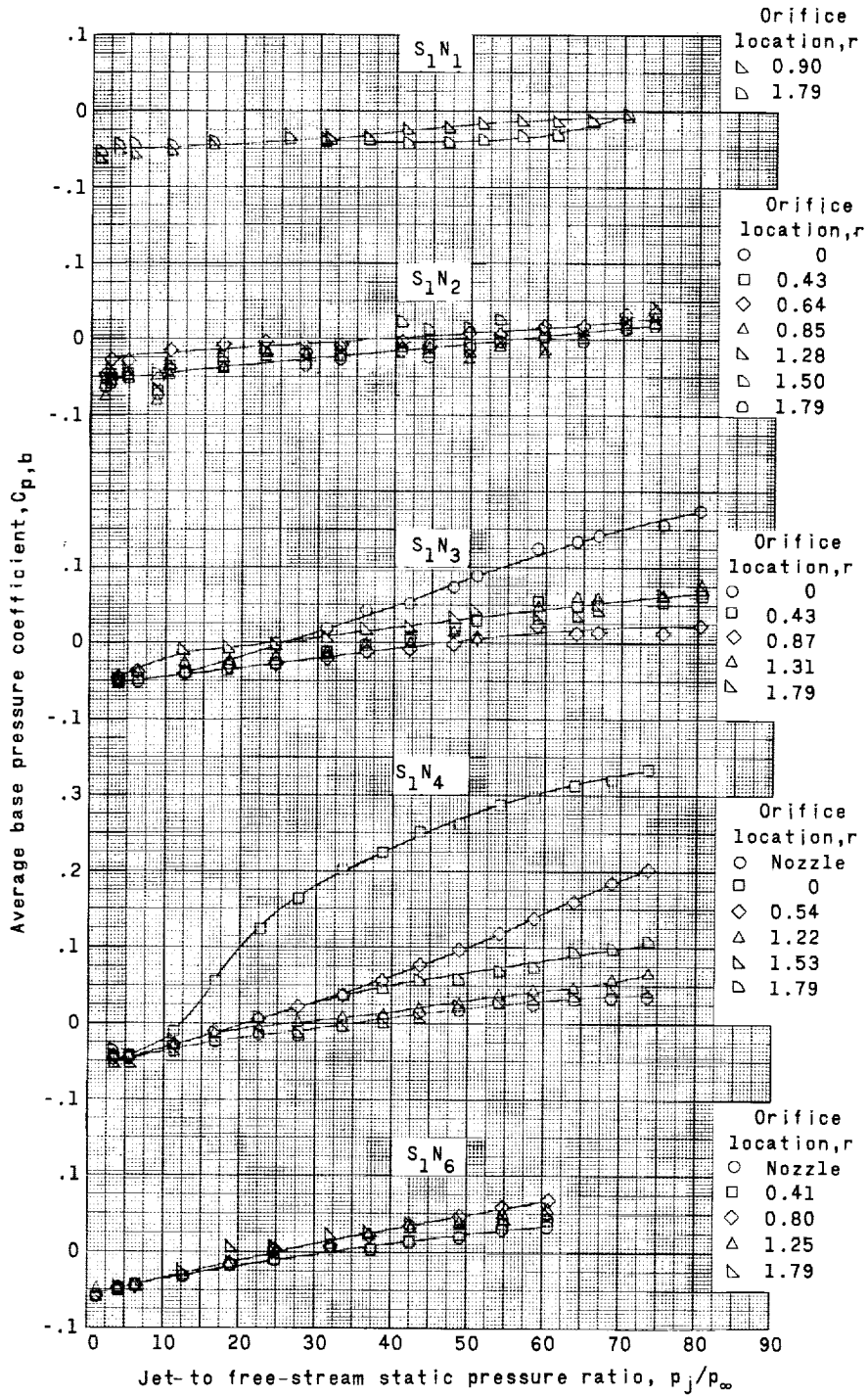

(c) $M_\infty = 4.00$.

Figure 10.- Continued.

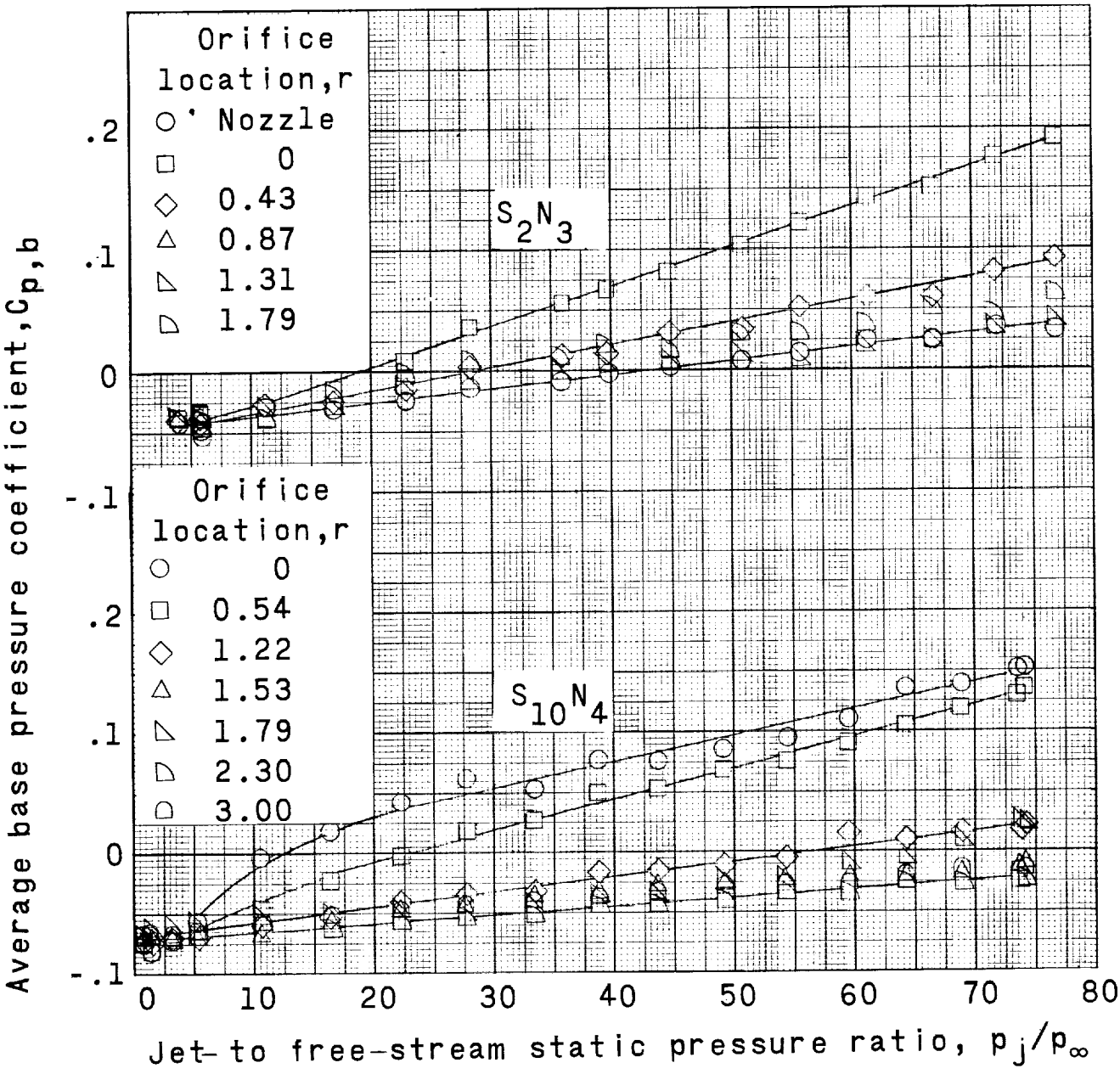

(c) Concluded.

Figure 10.- Continued.

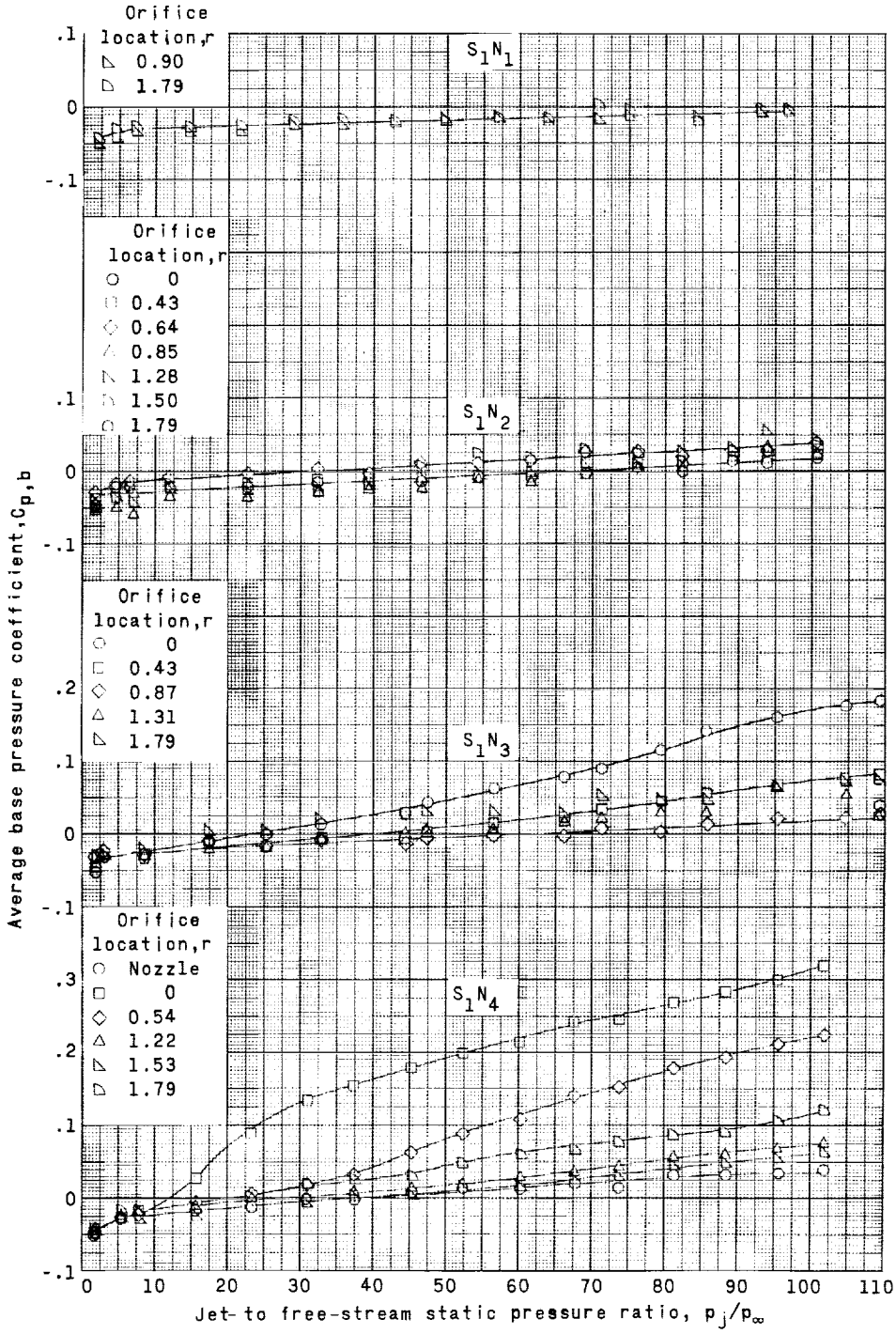

(d) $M_\infty = 4.65$.

Figure 10.- Continued.

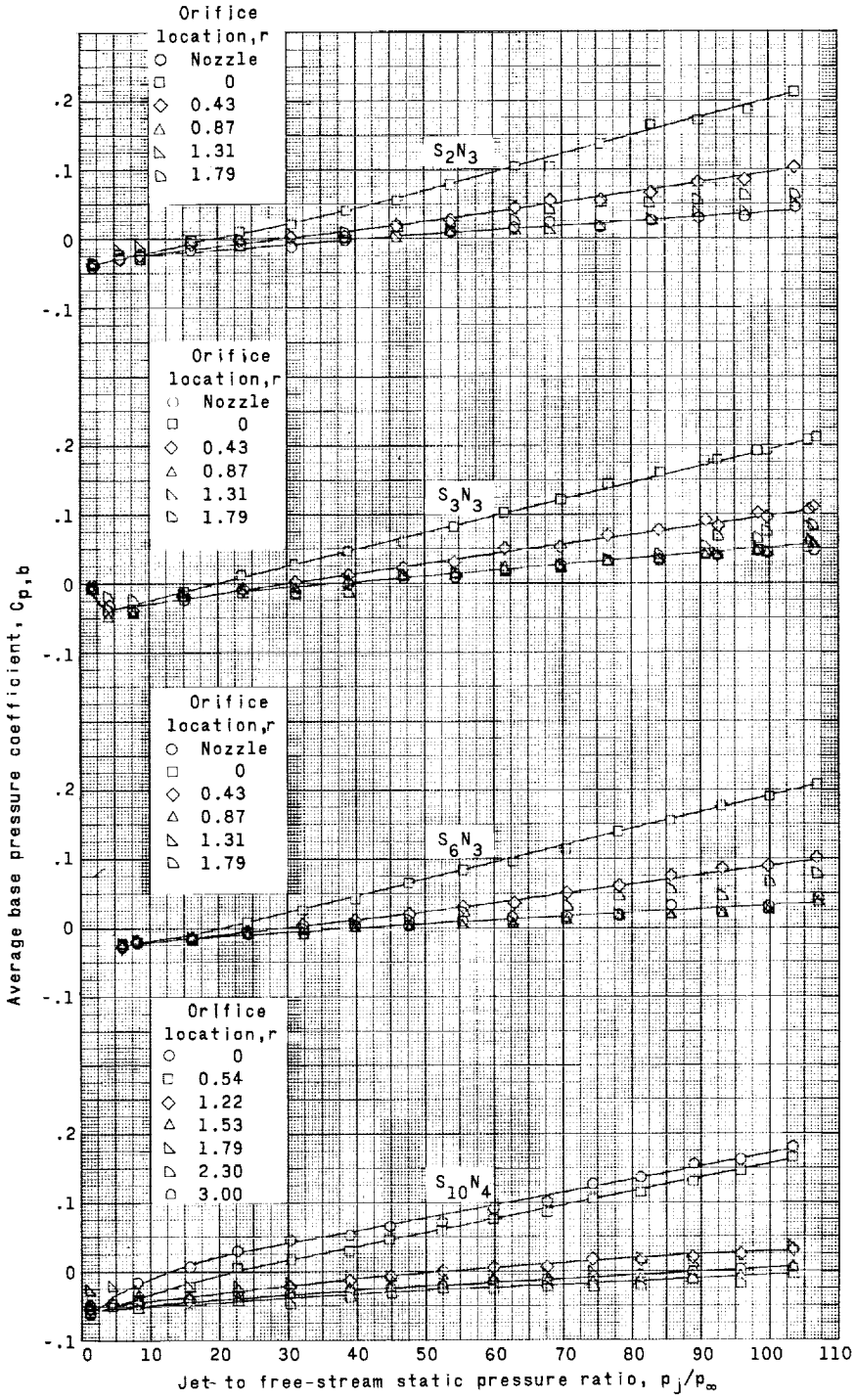

(d) Concluded.

Figure 10.- Concluded.

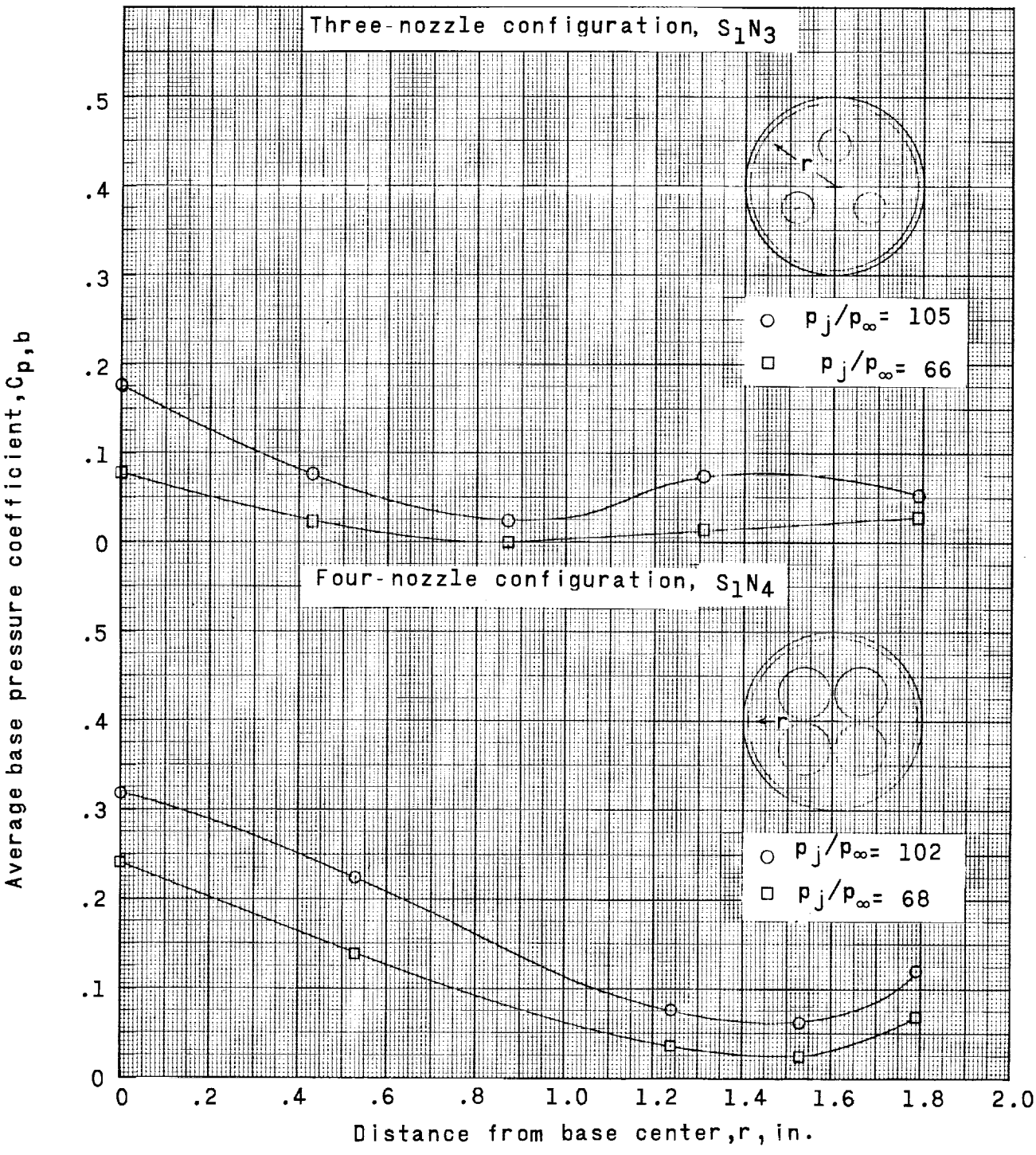

Figure 11.- Typical radial base-pressure distribution for three- and four-nozzle configurations. $M_\infty = 4.65$.

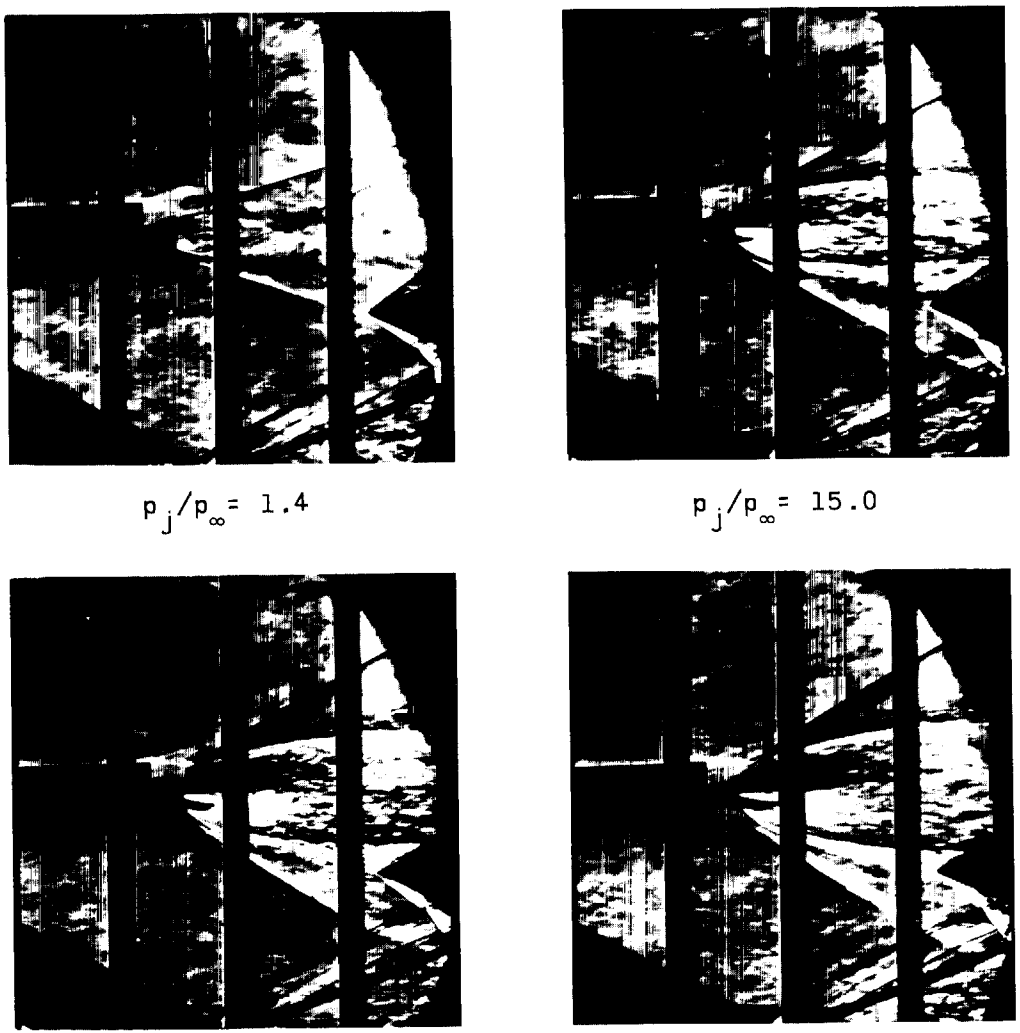

(a) Configuration S_1N_1; M_∞ = 2.95. L-63-4760

Figure 12.- Typical schlieren photographs of jet-exit flow with several combinations of base and skirt configurations.

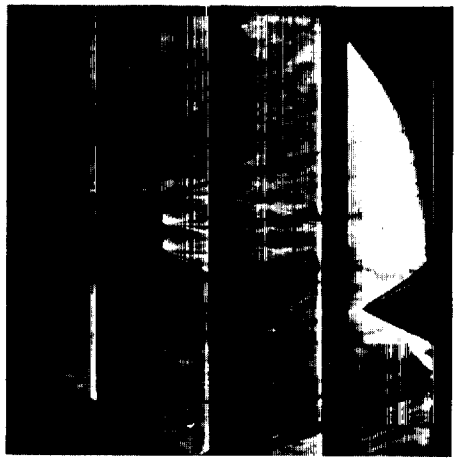

p_j/p_∞ = 2.7

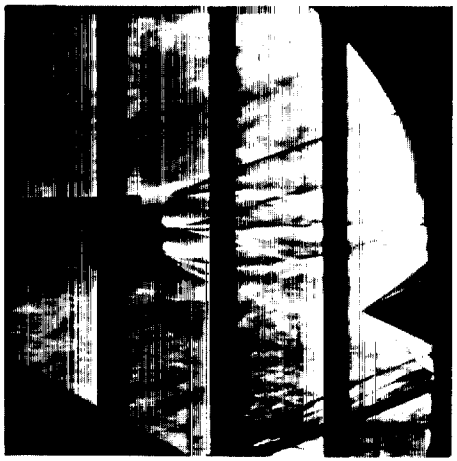

p_j/p_∞ = 10.4

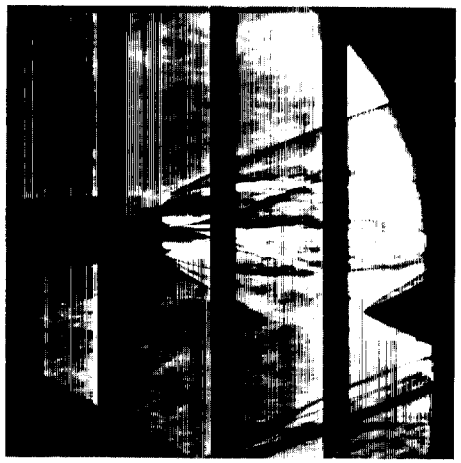

p_j/p_∞ = 22.7

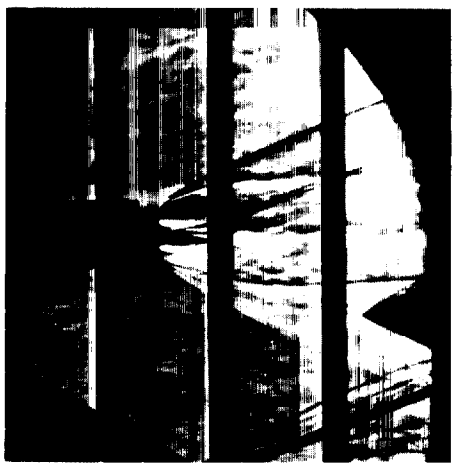

p_j/p_∞ = 32.6

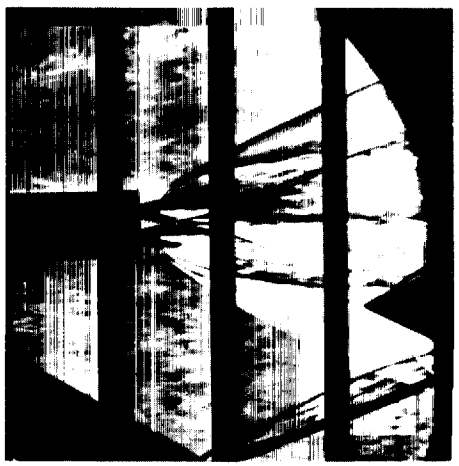

p_j/p_∞ = 53.8

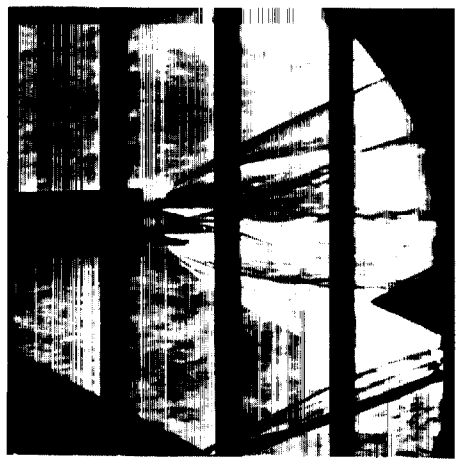

p_j/p_∞ = 64.8

(b) Configuration S_1N_2; M_∞ = 4.00.

L-63-4761

Figure 12.- Continued.

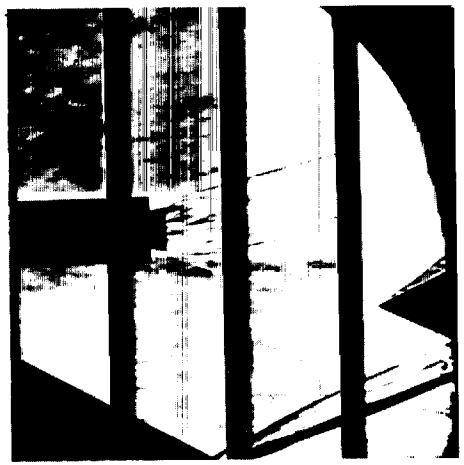

p_j/p_∞= 3.7

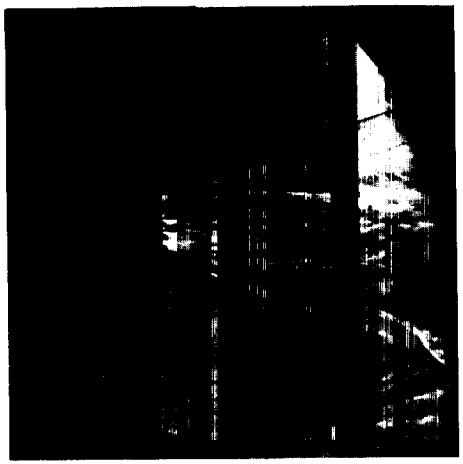

p_j/p_∞= 12.5

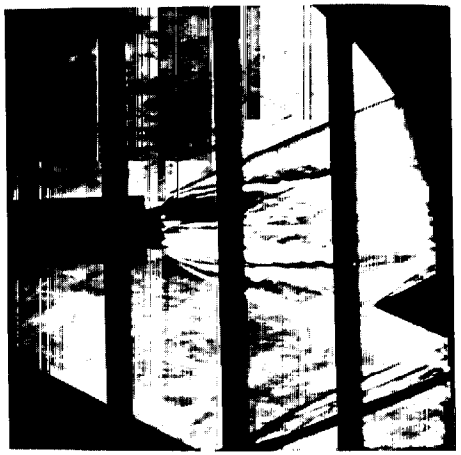

p_j/p_∞=24.5

p_j/p_∞= 47.9

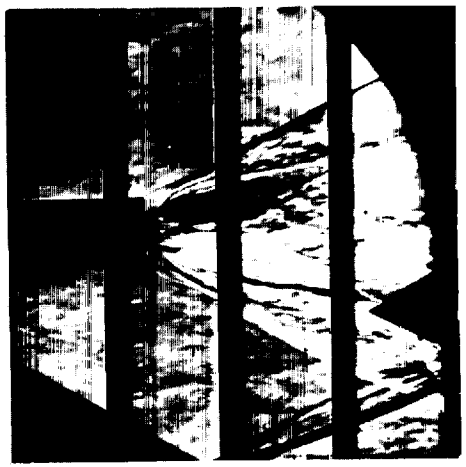

p_j/p_∞=66.9

p_j/p_∞=80.2

(c) Configuration S_1N_3; M_∞ = 4.00.

L-63-4762

Figure 12.- Continued.

p_j/p_∞= 3.5

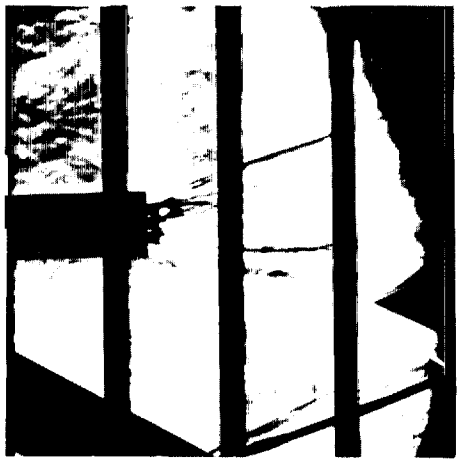

p_j/p_∞= 11.5

p_j/p_∞= 22.5

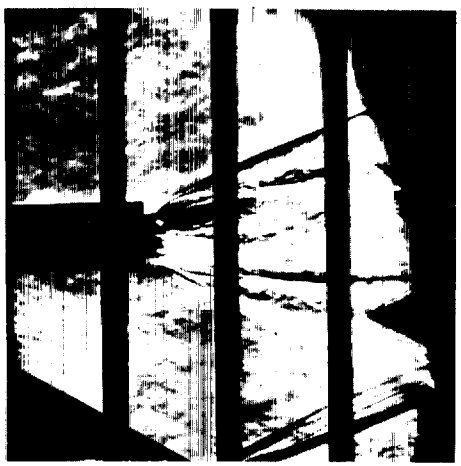

p_j/p_∞= 33.4

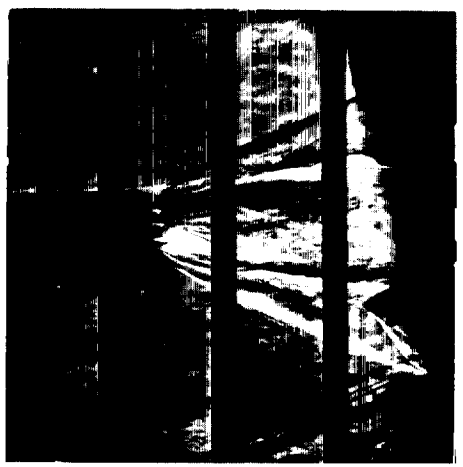

p_j/p_∞= 43.6

p_j/p_∞= 54.1

(d) Configuration S_1N_4; M_∞ = 4.00.

L-63-4763

Figure 12.- Continued.

p_j/p_∞= 2.0

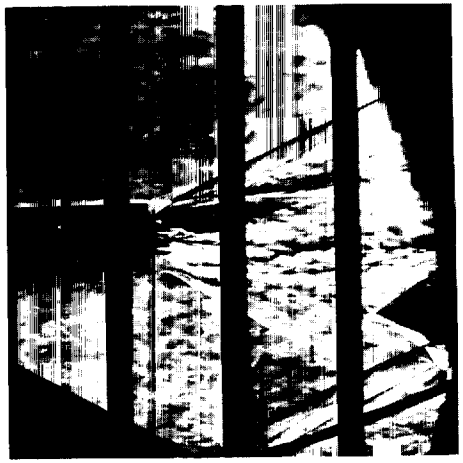

p_j/p_∞= 18.0

p_j/p_∞=29.2

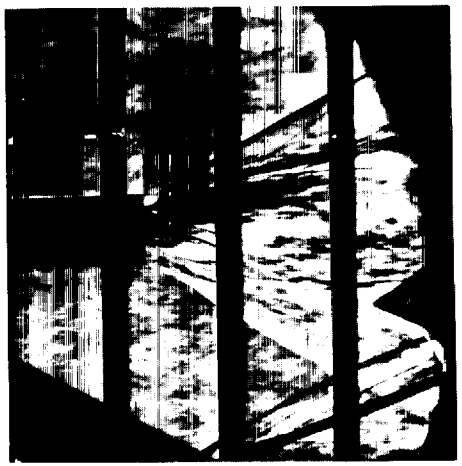

p_j/p_∞= 38.7

(e) Configuration S_1N_6; M_∞ = 2.95. L-63-4764

Figure 12.- Continued.

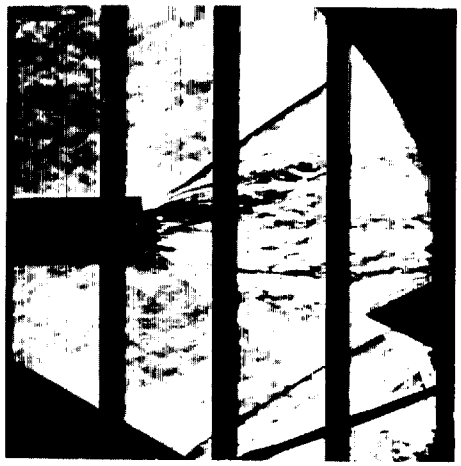

M_∞= 2.30

M_∞= 2.95

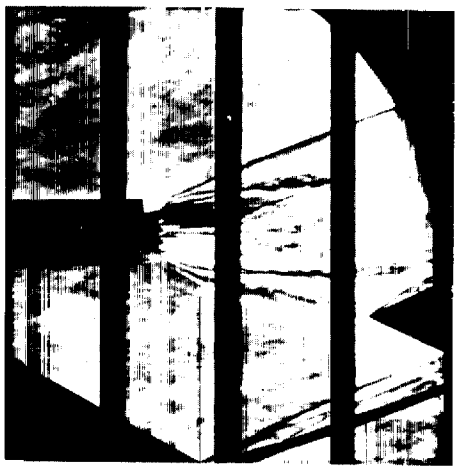

M_∞= 4.00

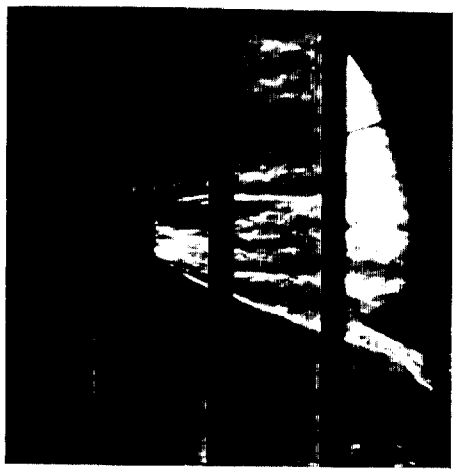

M_∞= 4.65

(f) Configuration S_1N_3; $p_j/p_\infty \approx 20$. L-63-4765

Figure 12.- Continued.

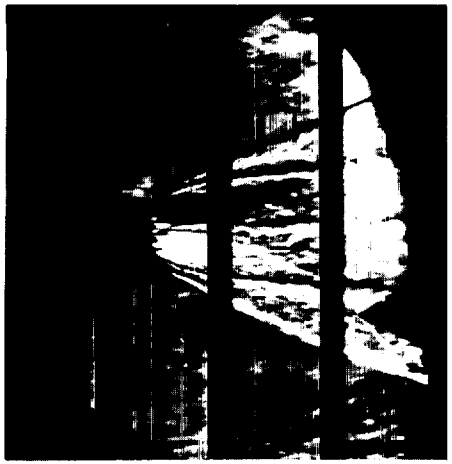

$S_1, p_j p/_\infty = 47.3$

$S_2, p_j/p_\infty = 46.1$

$S_3, p_j/p_\infty = 46.8$

$S_1, p_j/p_\infty = 95.2$

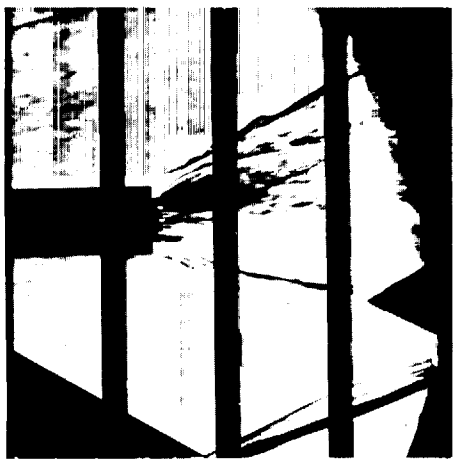

$S_2, p_j/p_\infty = 103.7$

$S_3, p_j/p_\infty = 105.1$

(g) Configuration N_3; $M_\infty = 4.65$.

L-63-4766

Figure 12.- Continued.

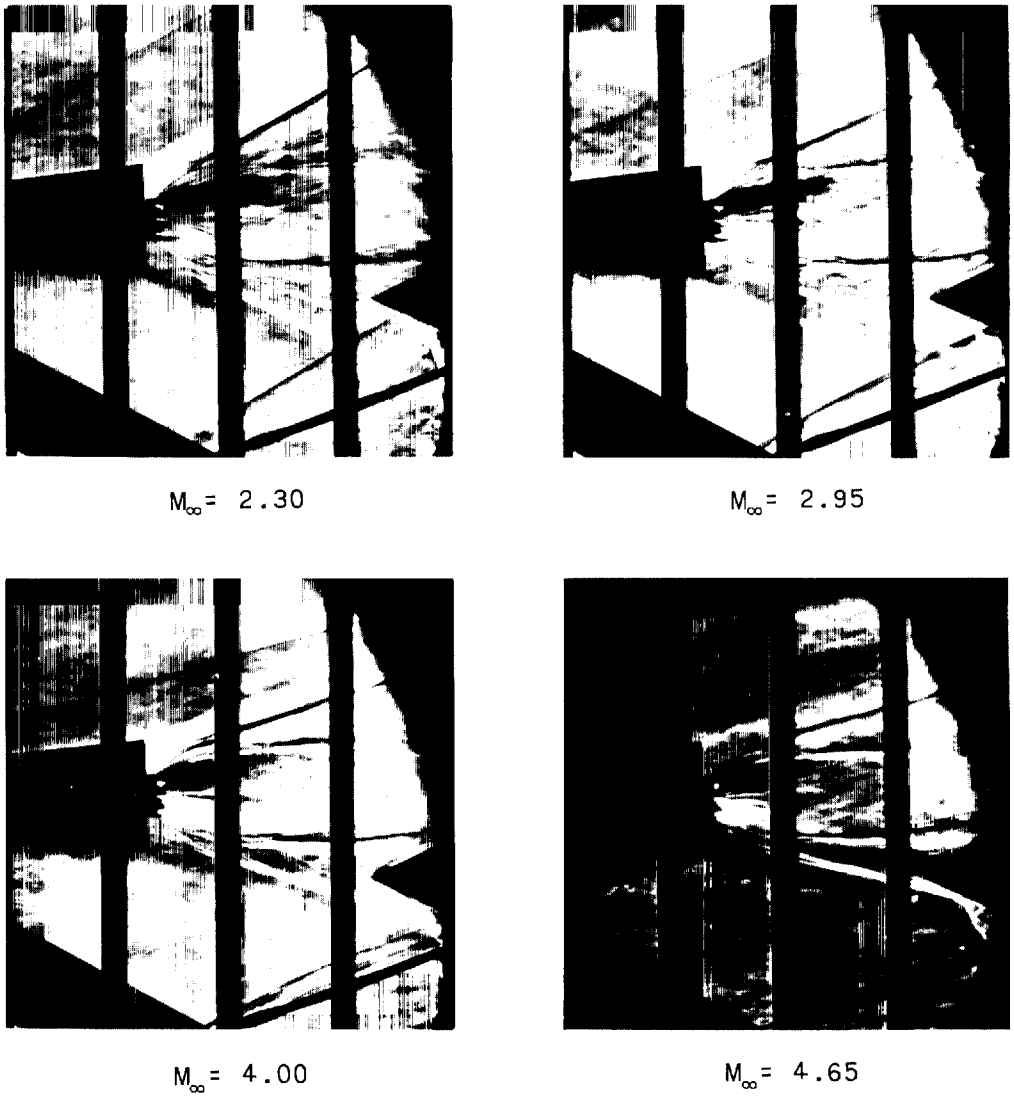

(h) Configuration $S_{10}N_4$; $p_j/p_\infty \approx 20$. L-63-4767

Figure 12.- Concluded.